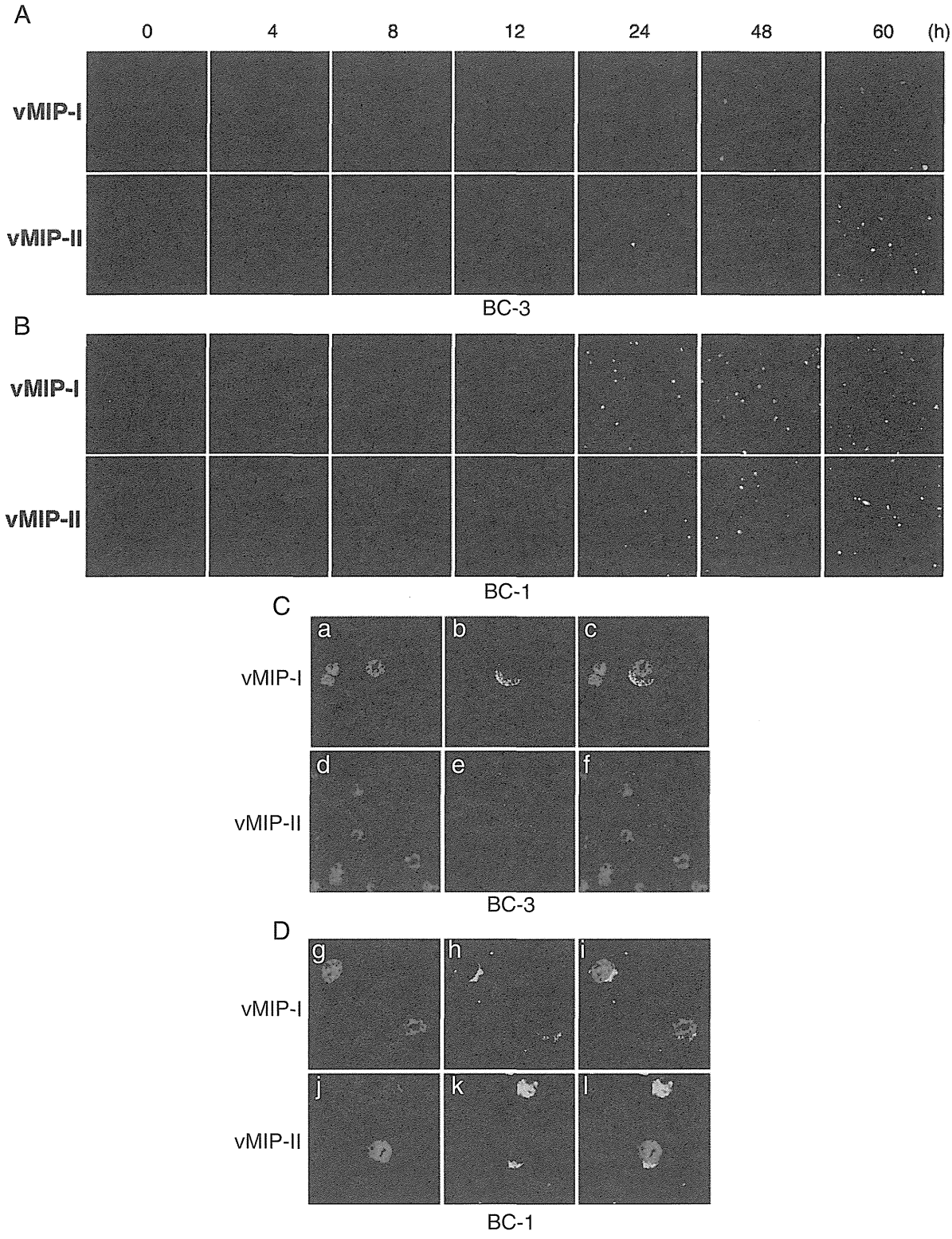

Fig. 4. Expression of vMIP-I and vMIP-II in BC-3 and BC-1 cells by IFA. After 4, 8, 12, 24, 48, and 60 h, BC-3 (A) and BC-1 (B) cells were labeled either with the anti-vMIP-I (upper) or the anti-vMIP-II (lower) MAb followed by goat anti-mouse FITC-conjugated Abs. FITC photomicrographs showing anti-vMIP-I and anti-vMIP-II immunoreactivity in BC-3 and BC-1 cells treated with TPA. (C) Cellular localization of vMIP-I and vMIP-II in BC-3 (C) and BC-1 (D) cells. The cells were stained with DAPI (a, d, g and j), and the localization of vMIP-I and vMIP-II was visualized by IFA with anti-vMIP-I or -vMIP-II MAbs (b, e, h and k); panel a and b, d and e, g and h, and j and k were merged (c, f, i and l). Fluorescence photomicrographs revealed anti-vMIP-I and -vMIP-II immunoreactivity using FITC-conjugated anti-mouse IgG MAb.

anti-mouse or rabbit antibodies (Invitrogen) were used as the secondary antibodies. Confocal microscopic analysis was performed (FV-1000, Olympus, Tokyo, Japan), and the contrast was adjusted before the images were exported as TIFF files to Adobe Photoshop.

Immunohistochemistry

Formalin-fixed paraffin-embedded tissues from KS and MCD patients, and those from an animal model of KSHV-associated solid lymphoma

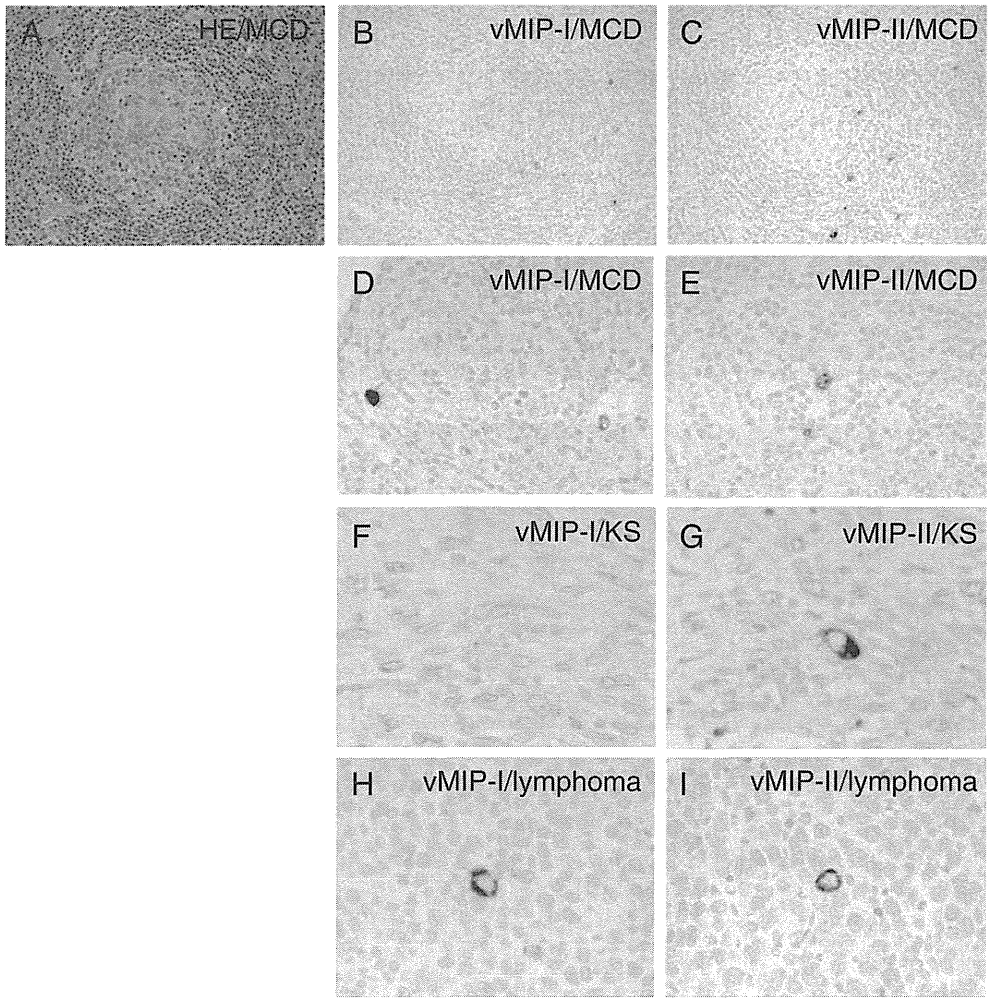

Fig. 5. Expression of vMIP proteins in KSHV-associated diseases. (A–C) Hematoxylin and eosin staining and immunohistochemistry for vMIPs in serial sections of a tissue sample from a patient with MCD. Brown stains indicate positive signals. The nucleus was counter-stained by hematoxylin. (D and E) Higher magnification view of vMIPs expression in an MCD case. Some large lymphocytes in the mantle zone were stained. (F and G) vMIP-I and vMIP-II expression in a KS sample. (H and I) Expression of vMIPs in an animal model of KSHV-associated lymphoma in SCID mice.

were sectioned and stained with hematoxylin and eosin (H&E). Immunohistochemistry of the serial sections was performed with either the anti-vMIP-I or -II MAb. For the second- and third- phase reagents used for immunostaining, a CSAII kit (DAKO, Copenhagen, Denmark) was used. An animal model of KSHV-associated solid lymphoma, which was established as described previously (Katano et al., 2000b), was also subjected to immunohistochemical analysis. Briefly, TY-1 cells were inoculated into the subcutaneous tissue of mice with severe combined immunodeficiency (SCID). One month after inoculation, lymphomas appeared in the subcutaneous region at the inoculation site. Lymphoma cells contained the KSHV genome, and expressed various viral proteins of KSHV (Katano et al., 2000b).

Table 1
Expression of vMIP-I and vMIP-II in MCD and KS tissue samples.

	KSHV proteins, (+)/total	
Cases	vMIP-I	vMIP-II
MCD	(3)/3	(3)/3
KS	(0)/5	(2)/8

Chemotaxis assays

Chemotaxis assays were performed as described previously (Nakano et al., 2003). Briefly, THP-1 cells were washed twice with chemotaxis buffer, 0.5% bovine serum albumin, 20 mM HEPES, pH 7.4, in RPMI 1640. Migration of cells was assessed in a cell culture chamber (Costar, Cambridge, MA), with the upper and lower compartments separated by a 3 μm pore size polycarbonate filter (???). The lower compartment of the chamber was filled with dilutions of vMIP-I, vMIP-II (R&D Systems, Minneapolis, MN) or with PBS alone, and/or with each 10 μg/ml anti-vMIP-I or -vMIP-II MAbs at a volume of 600 μl. The upper compartment contained 100 μl of THP-1 cell suspensions in chemotaxis buffer (10^5 cells/well). The chambers were then incubated for 4 hours at 37 °C, 5% CO_2, and spun at 300 x g, 4 °C, for 5 min. Finally, the cells from the lower compartment were counted.

Results

Specificity of the anti-vMIP-I MAb and the anti-vMIP-II MAb

In order to check specificity of the MAbs, we transfected vMIP-I and vMIP-II expression vectors (pCAGGS-vMIP-I, and -II) into 293/EBNA

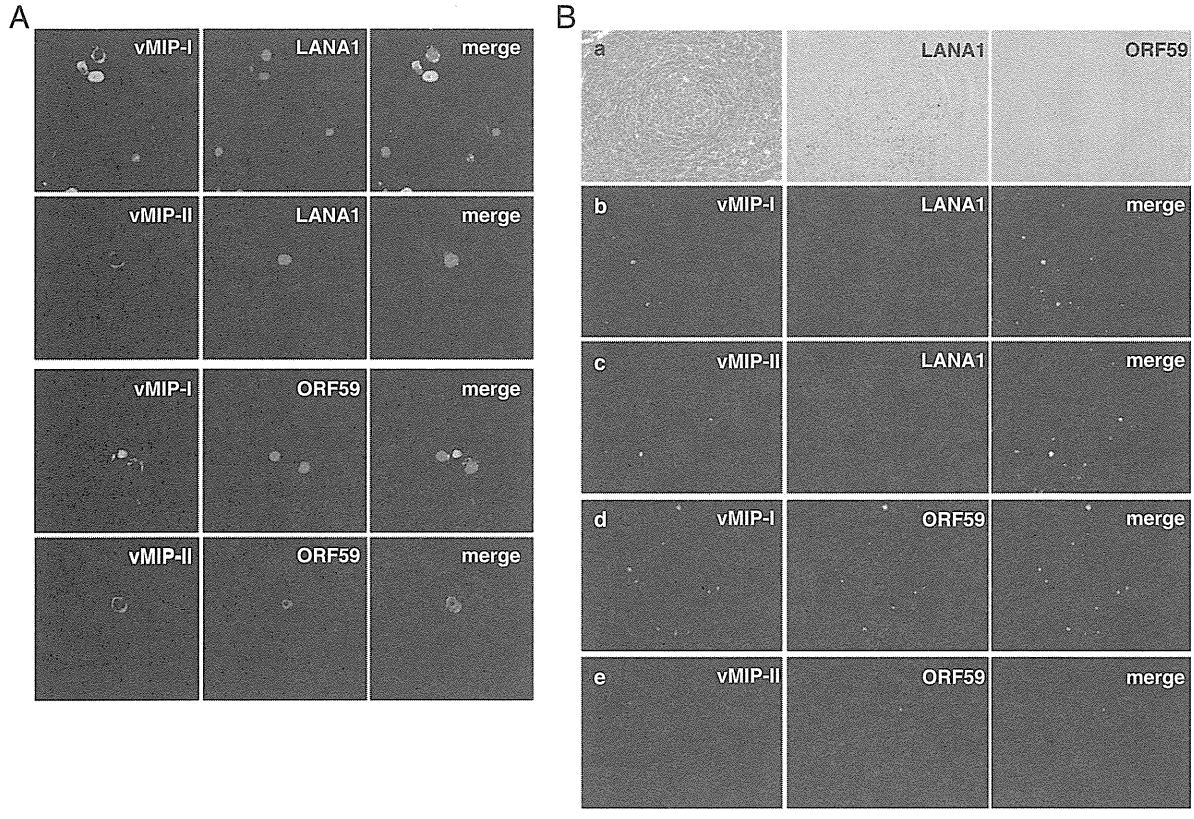

Fig. 6. (A) Expression of vMIPs. LANA1 and ORF59 in the animal model of KSHV-associated solid lymphoma by confocal microscopy. vMIPs were labeled with Alexa 488 (green). LANA1 (upper panels) and ORF59 (lower panels) were labeled with Alexa 568 (red). (B) Expression of vMIPs in MCD. (a) HE staining and immunohistochemistry of LANA1 and ORF59. (b–e) Immunofluorescence assay on MCD lesion. A germinal center is shown in the center of each panel. This case is KSHV-positive large B cell lymphoma arising in MCD (for interpretation of the color references in this article, the reader is referred to the online version).

cells, respectively. The total lysate of the transfected cells was subjected to Western blot analysis. vMIP-I and vMIP-II proteins were detected with anti-vMIP-I or vMIP-II MAbs, respectively (Fig. 1). These antibodies did not show cross-reactivity each other.

Epitope mapping of the anti-vMIP-I and anti-vMIP-II MAbs

We established hybridoma clones secreting MAbs against vMIP-I and vMIP-II, respectively. To map the regions of vMIP-I and vMIP-II where anti-vMIP-I and anti-vMIP-II antibody reacted, a series of GST-fused vMIP-I and vMIP-II deleted proteins were constructed as described in Fig. 2C and F, and used for Western blot analysis with an anti-GST antibody (Santa Cruz Biotechnology Inc), (Fig. 1A, D) and the anti-vMIP-I or the anti-vMIP-II (Fig. 1B, E) antibody, respectively. The results showed that all GST-vMIP-I and GST-vMIP-II fusion proteins interacted with the anti-GST antibody (Fig. 2A, D) and showed that GvM1-Full, GvM1-D1, and GvM1-D2 reacted with the anti-vMIP-I antibody, whereas GvM1-D3 did not (Fig. 1B), and GvM2-Full and GvM2-D1 reacted with the anti-vMIP-II antibody, whereas GvM2-D2, and GvM2-D3 did not (Fig. 2E). Thus, these results demonstrated that an anti-vMIP-I MAbs was successfully generated and suggest that the amino acid residues 61 to 95 of vMIP-I could be a major epitope reacted with the anti-vMIP-I antibody. On the other hand, the amino acid residues 24 to 42 of vMIP-II could be an epitope reacted with the anti-vMIP-II antibody.

Expression of vMIP-I and vMIP-II in the KSHV-infected PEL cell line

We tested vMIP-I and vMIP-II expression in KSHV and Epstein Barr virus (EBV) dually infected PEL cell lines (BC-1), KSHV infected PEL cell lines (BC-3) and in non-infected Burkitt's lymphoma cell line (BJAB), and detected them in TPA-stimulated BC-3 and BC-1 cells with developed antibodies, but not in BJAB cells non-stimulated BC-3 or BC-1 cells (Fig. 2A, B). In a KSHV infected PEL cells, BC-1 and BC-3, vMIP-I and vMIP-II were detected around at 10 kDa, which matches the size deduced from amino acids length (Fig. 3C, D). Actually, vMIP-I was detected from 6 hours post induction and vMIP-II was at 24 hours in BC-3 cells (Fig. 3C), and vMIP-I and vMIP-II were detected at 24 h in BC-1 cells (Fig. 3D). In the immunofluorescence microscopy, the number of vMIP-II expressing cells seemed to be more than that of vMIP-I in BC-3 cells (Fig. 4A, B). In order to analyze the cellular localization of vMIP-I and vMIP-II protein, BC-3 and BC-1 cells stimulated with TPA were doubly labeled with DAPI (Fig. 4C, a, d and D, g, j), and either the anti-vMIP-I MAb (Fig. 4C, b and D, h) or the anti-vMIP-II MAb (Fig. 4C, e and D, k). Merged images were shown in Fig. 4C, c, f, and D, i, l). The vMIP-I and the vMIP-II clearly showed cytoplasm and possibly membranes in TPA-induced BC-3 and BC-1 cells (Fig. 4C, b, e, and D, h, k).

Expression of vMIPs in KSHV-associated diseases

To know the expression of vMIPs in KSHV-associated diseases, immunohistochemistry for vMIPs was performed on pathological samples of eight KS cases, three MCD cases, and the animal model of KSHV-associated solid lymphoma (Fig. 5). Immunohistochemistry demonstrated that vMIP-I and vMIP-II were detected in some cells in the mantle zone of germinal center and the interfollicular zone in KSHV-positive MCD samples (Fig. 5A to E). Both vMIP-I and vMIP-II were detected predominantly in the cytoplasm of large lymphocytes. The numbers of positive cells varied among three MCD cases examined. On the other

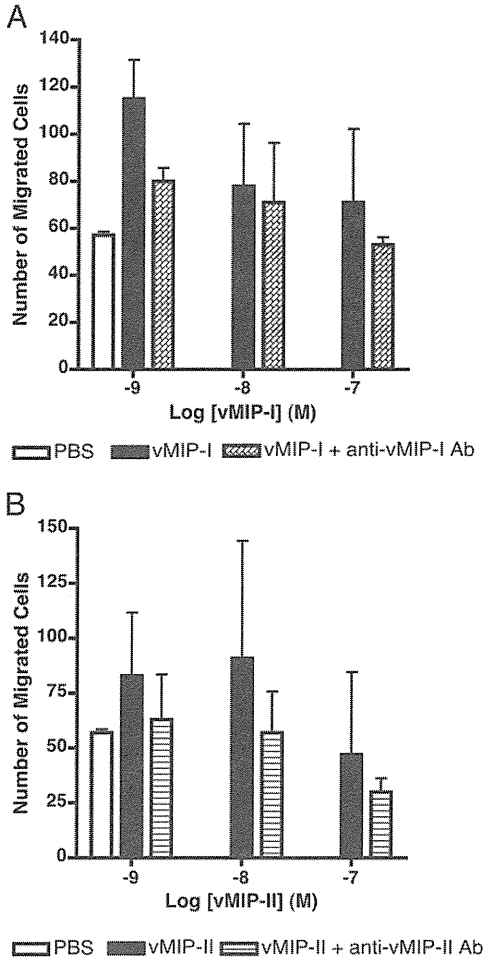

Fig. 7. Neutralizing activity of anti-vMIP-I and -vMIP-II MAbs. THP-1 cell migration in response to increased concentrations of vMIP-I and vMIP-II (1, 10, 100 nM), and the neutralizing activity of 10 μg/ml anti-vMIP-I and -vMIP-II MAbs against vMIP-I and vMIP-II were measured, as outlined in Materials and Methods, by using the transwell migration assay system. Various doses of vMIP-I and vMIP-II were tested for their ability to induce the chemotaxis of THP-1 cells. The data presented are from one experiment, and are representative of the triplicate experiments performed. The error bars indicate the standard deviations of three independent experiments.

hand, any positive signal of vMIP-I was not observed in all KS cases (Fig. 5F, G). vMIP-II was rarely detected in the cytoplasm of spindle cells in two KS cases at the nodular stage out of eight KS cases. In the samples of animal model of KSHV-associated solid lymphoma, both vMIP-I and vMIP-II were detected in the cytoplasm of a part of lymphoma cells (Fig. 5H, I). These data showed that vMIP-I and vMIP-II were expressed in cells in MCD and KSHV-associated lymphoma, but vMIP-II was rarely in KS (Table 1). To know the association of vMIPs expression with expression of other KSHV-encoded proteins, we examined immunofluorescence assay on KSHV-associated diseases. Since, all KSHV-infected cells express LANA1, vMIPs-positive cells were positive for LANA1. However, expression pattern of LANA1 showed diffuse nuclear staining in vMIPs-positive cells in the animal model of KSHV-associated solid lymphoma (Fig. 6A). Confocal microscopy revealed that vMIP-I stain showed usually cytoplasmic pattern, but rarely diffuse nuclear staining pattern *in vivo*. Almost all cells with vMIPs expression were also positive for ORF59 protein, a lytic protein of KSHV. IFA also demonstrated that vMIPs-positive cells expressed LANA1 at various levels in MCD clinical samples (Fig. 6B, a to c). A large portion of vMIPs-positive cells also expressed ORF59 protein in MCD (Fig. 6B, d, e). These data suggest that vMIPs are expressed by cells with KSHV-lytic infection in KSHV-associated MCD and lymphoma.

Neutralization of vMIP-I and vMIP-II by anti-vMIP-I and anti-vMIP-II MAbs

We examined whether the anti-vMIP-I and anti-vMIP-II MAbs could neutralize the chemoattractant of vMIP-I and vMIP-II to induce the migration of THP-1 cells. As expected, vMIP-I and vMIP-II induced migration of THP-1 cells (Fig. 7A, B), but not with PBS alone. However, anti-vMIP-I and anti-vMIP-II MAbs inhibited respective vMIP-I and vMIP-II-induced cell migration of THP-1 cells at 10 μg/ml final concentration.

Discussions

It was known that KSHV encodes three chemokine genes of the so-called viral macrophage inflammatory proteins: *vMIP-I*, *vMIP-II*, and *vMIP-III* in the genome. Analysis of the translated amino acid sequence indicate that the vMIP-I and vMIP-II gene have four conserved cysteines capable of forming two essential disulfide bonds (first cysteine and third cysteine, and second cysteine and fourth cysteine). The family of chemokines comprises CC, CXC, C, and CX_3C subfamilies. The vMIP-I and vMIP-II have four cysteines, the first two of which are found in the sequence of CC, which correspond to the CC profile. These gene products were expressed in the phase of KSHV lytic infection (Moore et al., 1996; Sun et al., 1999). Both vMIP-I and vMIP-II were expressed in a KSHV-infected cell lines, BC-3, which had been treated with TPA. Mono-specific polyclonal Abs against vMIP-I and vMIP-II have been described in previous studies that investigated the localization of vMIPs in PEL cells (Nakano et al., 2003). In the present study, we developed the respective MAbs that reacted either with KSHV vMIP-I or vMIP-II. We first applied these MAbs against KSHV vMIP-I and vMIP-II to detect KSHV-infected BC-3 and BC-1 cells by Western blotting and immunofluorescence assay. The Western blot analysis revealed that both the anti-vMIP-I and the anti-vMIP-II MAbs reacted to the 10-kDa proteins considered specific to the respective vMIP protein. The anti-vMIP-I MAb was shown to be reactive with the epitopes in the middle of the protein (sequence, PPVQILKEWYPTSPAC), and the epitope of the anti-vMIP-II MAb was shown to be reactive at the N-terminal end (sequence, LGASWHRPDKCCLGYQKRP). Further immunofluorescence analysis of the cellular localization of both vMIP-I and vMIP-II with anti-vMIP-I and anti-vMIP-II MAb showed a cytoplasmic pattern of expression in BC-3 and BC-1 cells. As the results indicated that these gene products were expressed in the cytoplasm, it might be located at the KSHV-infected BC-3 or BC-1 cells membrane prior to secretion. An investigation of the antigenic specificities of MAbs against KSHV vMIP-I and vMIP-II in MCD and KS patients has not yet been reported. Here, immunohistochemical analysis detected only vMIP-II in samples from both KS and MCD patients, but vMIP-I was not detected in KS cases: however, both vMIP-I and vMIP-II proteins were expressed in some cells in the interfollicular zone of MCD tissues. Lytic proteins of the KSHV such as K8, RTA, and ORF59 have been detected in large lymphocytes in the mantle zone of MCD cases (Dupin et al., 1999; Katano et al., 2000a). The expression of vMIPs showed a similar pattern to that of the lytic proteins in MCD tissues. In contrast, lytic protein expression, including that of vMIPs, was rare in the KS lesions (Abe et al., 2006). In the present study, we demonstrated that vMIPs were expressed in the cells expressing ORF59 protein. Thus, our data clearly indicated that the expression of vMIPs is associated with lytic infection in individual cells affected by KSHV-associated diseases. Human monocytic cell line THP-1 respond to various chemokines suggesting that they express receptors for these chemokines (Wang et al., 1993). Previous study, vMIP-I and vMIP-II were shown chemotaxis in THP-1 cells (Nakano et al., 2003). It has been reported that vMIP-I acts as a specific agonist for CC chemokine receptor 8 (CCR8) (Dairaghi et al., 1999; Endres et al., 1999) and vMIP-II shows a Ca^{2+} flux as a specific agonist for CCR3 (Boshoff et al., 1997). Our data showed anti-vMIP-I and anti-vMIP-II MAbs were able to neutralize vMIP-I- and vMIP-II-mediated chemotaxis in THP-1 cells. However, neutralizing activities

ARTICLE IN PRESS

of anti-vMIP-I MAb was apparently low, even the addition of 10 μg/ml MAbs. These findings support the assumption that anti-vMIP-I and –vMIP-II MAbs-blocked chemotaxis in THP-1 cells act through binding to the certain amino acid residue of vMIP-I and vMIP-II.

In summary, MAbs developed specifically for this series were used to detect vMIP-I and vMIP-II in MCD and KS tissues, which may account for certain clinical features of MCD and KS. To gain a better understanding of these important viral genes, additional studies will be needed that focus on revealing vMIP-I and vMIP-II expression profiles during lytic infection. Taken together, these studies provide an insight into the pathogenesis of the contribution of vMIP-I and vMIP-II to the lytic induction of KSHV. These MAbs could serve as useful tools to clarify the pathogenesis of KSHV-related diseases.

Acknowledgments

This study was supported by a grant for Research on Publicly Essential Drugs and Medical Devices from the Japan Health Sciences Foundation (SAA4832), Health and Labor Sciences Research Grants (to HK, No. H23-AIDS-Ippan-002) from the Ministry of Health and by a grant from PRESTO of the Japan Science and Technology Corporation (200154023).

References

Abe, Y., Matsubara, D., Gatanaga, H., Oka, S., Kimura, S., Sasao, Y., Saitoh, K., Fujii, T., Sato, Y., Sata, T., Katano, H., 2006. Distinct expression of Kaposi's sarcoma-associated herpesvirus-encoded proteins in Kaposi's sarcoma and multicentric Castleman's disease. Pathol. Int. 56, 617–624.

Arvanitakis, L., Mesri, E.A., Nador, R.G., Said, J.W., Asch, A.S., Knowles, D.M., Cesarman, E., 1996. Establishment and characterization of a primary effusion (body cavity-based) lymphoma cell line (BC-3) harboring kaposi's sarcoma-associated herpesvirus (KSHV/HHV-8) in the absence of Epstein-Barr virus. Blood 88, 2648–2654.

Benelli, R., Barbero, A., Buffa, A., Aluigi, M.G., Masiello, L., Morbidelli, L., Ziche, M., Albini, A., Noonan, D., 2000. Distinct chemotactic and angiogenic activities of peptides derived from Kaposi's sarcoma virus encoded chemokines. Int. J. Oncol. 17, 75–81.

Boshoff, C., Endo, Y., Collins, P.D., Takeuchi, Y., Reeves, J.D., Schweickart, V.L., Siani, M.A., Sasaki, T., Williams, T.J., Gray, P.W., Moore, P.S., Chang, Y., Weiss, R.A., 1997. Angiogenic and HIV-inhibitory functions of KSHV-encoded chemokines. Science 278, 290–294.

Cesarman, E., Chang, Y., Moore, P.S., Said, J.W., Knowles, D.M., 1995. Kaposi's sarcoma-associated herpesvirus-like DNA sequences in AIDS-related body-cavity-based lymphomas. N. Engl. J. Med. 332, 1186–1191.

Chang, Y., Cesarman, E., Pessin, M.S., Lee, F., Culpepper, J., Knowles, D.M., Moore, P.S., 1994. Identification of herpesvirus-like DNA sequences in AIDS-associated Kaposi's sarcoma. Science 266, 1865–1869.

Chen, S., Bacon, K.B., Li, L., Garcia, G.E., Xia, Y., Lo, D., Thompson, D.A., Siani, M.A., Yamamoto, T., Harrison, J.K., Feng, L., 1998. In vivo inhibition of CC and CX3C chemokine-induced leukocyte infiltration and attenuation of glomerulonephritis in Wistar–Kyoto (WKY) rats by vMIP-II. J. Exp. Med. 188, 193–198.

Dairaghi, D.J., Fan, R.A., McMaster, B.E., Hanley, M.R., Schall, T.J., 1999. HHV8-encoded vMIP-I selectively engages chemokine receptor CCR8. Agonist and antagonist profiles of viral chemokines. Biol. Chem. 274, 21569–21574.

Dupin, N., Fisher, C., Kellam, P., Ariad, S., Tulliez, M., Franck, N., van Marck, E., Salmon, D., Gorin, I., Escande, J.P., Weiss, R.A., Alitalo, K., Boshoff, C., 1999. Distribution of human herpesvirus-8 latently infected cells in Kaposi's sarcoma, multicentric Castleman's disease, and primary effusion lymphoma. Proc. Natl. Acad. Sci. U. S. A. 96, 4546–4551.

Endres, M.J., Garlisi, C.G., Xiao, H., Shan, L., Hedrick, J.A., 1999. The Kaposi's sarcoma-related herpesvirus (KSHV)-encoded chemokine vMIP-I is a specific agonist for the CC chemokine receptor (CCR)8. J. Exp. Med. 189, 1993–1998.

Katano, H., Sato, Y., Kurata, T., Mori, S., Sata, T., 2000a. Expression and localization of human herpesvirus 8-encoded proteins in primary effusion lymphoma, Kaposi's sarcoma, and multicentric Castleman's disease. Virology 269, 335–344.

Katano, H., Suda, T., Morishita, Y., Yamamoto, K., Hoshino, Y., Nakamura, K., Tachikawa, N., Sata, T., Hamaguchi, H., Iwamoto, A., Mori, S., 2000b. Human herpesvirus 8-associated solid lymphomas that occur in AIDS patients take anaplastic large cell morphology. Mod. Pathol. 13, 77–85.

Kledal, T.N., Rosenkilde, M.M., Coulin, F., Simmons, G., Johnsen, A.H., Alouani, S., Power, C.A., Luttichau, H.R., Gerstoft, J., Clapham, P.R., Clark-Lewis, I., Wells, T.N., Schwartz, T.W., 1997. A broad-spectrum chemokine antagonist encoded by Kaposi's sarcoma-associated herpesvirus. Science 277, 1656–1659.

Miller, G., Heston, L., Grogan, E., Gradoville, L., Rigsby, M., Sun, R., Shedd, D., Kushnaryov, V.M., Grossberg, S., Chang, Y., 1997. Selective switch between latency and lytic replication of Kaposi's sarcoma herpesvirus and Epstein-Barr virus in dually infected body cavity lymphoma cells. J. Virol. 71, 314–324.

Moore, P.S., Boshoff, C., Weiss, R.A., Chang, Y., 1996. Molecular mimicry of human cytokine and cytokine response pathway genes by KSHV. Science 274, 1739–1744.

Nakano, K., Isegawa, Y., Zou, P., Tadagaki, K., Inagi, R., Yamanishi, K., 2003. Kaposi's sarcoma-associated herpesvirus (KSHV)-encoded vMIP-I and vMIP-II induce signal transduction and chemotaxis in monocytic cells. Arch. Virol. 148, 871–890.

Niwa, H., Yamamura, K., Miyazaki, J., 1991. Efficient selection for high-expression transfectants with a novel eukaryotic vector. Gene 108, 193–199.

Schalling, M., Ekman, M., Kaaya, E.E., Linde, A., Biberfeld, P., 1995. A role for a new herpes virus (KSHV) in different forms of Kaposi's sarcoma. Nat. Med. 1, 707–708.

Soulier, J., Grollet, L., Oksenhendler, E., Cacoub, P., Cazals-Hatem, D., Babinet, P., d'Agay, M.F., Clauvel, J.P., Raphael, M., Degos, L., et al., 1995. Kaposi's sarcoma-associated herpesvirus-like DNA sequences in multicentric Castleman's disease. Blood 86, 1276–1280.

Sun, R., Lin, S.F., Staskus, K., Gradoville, L., Grogan, E., Haase, A., Miller, G., 1999. Kinetics of Kaposi's sarcoma-associated herpesvirus gene expression. J. Virol. 73, 2232–2242.

Wang, J.M., McVicar, D.W., Oppenheim, J.J., Kelvin, D.J., 1993. Identification of RANTES receptor on human monocytic cells: competition of binding and desensitization by homologous chemotactic cytokines. J. Exp. Med. 177, 699–705.

Cancer Science
The official journal of the Japanese Cancer Association JCA

Antitumor effect of berberine against primary effusion lymphoma via inhibition of NF-κB pathway

Hiroki Goto,[1] Ryusho Kariya,[1] Masako Shimamoto,[1] Eriko Kudo,[1] Manabu Taura,[1] Harutaka Katano[2] and Seiji Okada[1,3]

[1]Division of Hematopoiesis, Center for AIDS Research, Kumamoto University, Kumamoto; [2]Department of Pathology, National Institute of Infectious Diseases, Tokyo, Japan

(Received September 1, 2011/Revised December 15, 2011/Accepted January 4, 2012/Accepted manuscript online February 9, 2012/Article first published online February 21, 2012)

Primary effusion lymphoma (PEL) is an infrequent and distinct entity among the aggressive non-Hodgkin B cell lymphomas that occurs predominantly in patients with advanced AIDS. It shows serous lymphomatous effusion in body cavities, and is resistant to conventional chemotherapy with a poor prognosis. Thus, the optimal treatment for PEL is not well defined and there is a need for novel agents. PEL has been recognized as the tumor caused by Kaposi sarcoma-associated herpes virus/human herpes virus-8 (KSHV/HHV-8), and nuclear factor (NF)-κB activation plays a critical role in the survival and growth of PEL cells. In this study, we assessed the antitumor effect of berberine, a naturally occurring isoquinoline alkaloid, on this pathway. The methylthiotetrazole assay showed that cell proliferation in the PEL cell lines was inhibited by berberine. Berberine also induced caspase-dependent apoptosis and suppressed NF-κB activity by inhibiting IκB kinase (IKK) phosphorylation, IκB phosphorylation and IκB degradation, upstream targets of the NF-κB pathway, in PEL cells. In a xenograft mouse model that showed ascites and diffuse organ invasion of PEL cells, treatment with berberine inhibited the growth and invasion of PEL cells significantly compared with untreated mice. These results show that the suppression of NF-κB is a molecular target for treating PEL, and berberine is a potential antitumor agent for PEL. (*Cancer Sci* 2012; 103: 775–781)

Primary effusion lymphoma (PEL) is a rare and distinct subtype of non-Hodgkin lymphoma that was originally identified in patients with advanced AIDS.[1,2] PEL arises exclusively in body cavities (pleura, peritoneum and pericardium) and is caused by Kaposi sarcoma-associated herpes virus/human herpes virus-8 (KSHV/HHV-8).[2] It is generally resistant to chemotherapy, with a median survival of only 3 months;[3] therefore, there is a need to develop new therapies. PEL displays constitutive activity of many signaling pathways in survival and growth, including the NF-κB, JAK/STAT and PI3K/Akt pathways.[4–6] Inhibition of NF-κB induces apoptosis in PEL cells and this pathway represents a molecular target for this disease.[4,7]

Berberine, an isoquinoline alkaloid from a plant used in traditional Chinese and Ayurvedic medicine, is an active component of *Berberis aquifolium* (Oregon grape), *Berberis aristata* (turmeric tree), *Berberis vulgaris* (barberry), *Coptis chinensis* (coptis or golden thread) and *Hydrastis canadensis* (golden seal). Berberine has a wide range of biological effects, including antidiarrheal, antihypertensive, antiarrhythmic, cholesterol-lowering, antimicrobial and anti-inflammatory activities.[8–13] In addition, berberine possesses antitumor activities against various tumor cells.[14–17] The suppression of NF-κB by berberine has been demonstrated in several tumor cell lines;[18–21] however, the specific target of the NF-κB pathway is not fully understood, and the antitumor ability *in vivo* of berberine is limited.[21–23] Further studies in animal models are required to identify the potential effects and clinical application of berberine.

In this study, we investigated the effect of berberine on proliferation and apoptosis in PEL cells and clarified the target molecules of berberine in the NF-κB pathway against PEL cells *in vitro*. The suppression of upstream molecules of the NF-κB pathway led to the inhibition of NF-κB activity. We also assessed the *in vivo* effect of berberine, showing the rationale for a clinical study. These findings provide insights into the molecular target of PEL and the antitumor mechanism of berberine against PEL cells.

Materials and Methods

Cell lines and reagents. Human PEL cell lines, BC-1,[24] BCBL-1,[25] TY-1[26] and human non-PEL cell line, U937,[27] were maintained in RPMI1640 supplemented with 10% heat-inactivated FCS, penicillin (100 U/mL) and streptomycin (100 μg/mL) in a humidified incubator at 37°C and 5% CO_2. Berberine chloride was obtained from Sigma-Aldrich (St. Louis, MO, USA).

Tetrazolium dye MTT assay. The antiproliferative activities of berberine against PEL cell lines were measured using the MTT method (Sigma-Aldrich). Briefly, 2×10^4 cells were incubated in triplicate in a 96-well microculture plate in the presence of different concentrations of berberine in a final volume of 0.1 mL for 24 h at 37°C. Subsequently, MTT (0.5 mg/mL final concentration) was added to each well. After 3 h of additional incubation, 100 μL of a solution containing 10% SDS plus 0.01 N HCl was added to dissolve the crystals. Absorption values at 595 nm were determined with an automatic ELISA plate reader (Multiskan; Thermo Electron, Vantaa, Finland). Values are normalized to untreated (control) samples.

Annexin V assay. Apoptosis was quantified using Annexin V-Alexa fluor 647 (AF647) (BioLegend, San Diego, CA, USA). Briefly, after treatment with berberine for 24 h, cells were harvested, washed and then incubated with Annexin V-AF647 for 60 min in the dark, before being analyzed on an LSR II cytometer (BD Bioscience, San Jose, CA, USA). Data were analyzed using FlowJo software (Tree Star, San Jose, CA, USA).

Analysis of DNA fragmentation by agarose gel electrophoresis. To detect apoptosis and DNA damage, DNA ladder assays were performed as previously described.[28] Briefly, BCBL-1 cells were cultured in the presence or absence of berberine at 37°C for 48 h. After incubation, 1×10^6 cells were lysed in 100 μL of 10 mM Tris–HCl buffer (pH 7.4)

[3]To whom correspondence should be addressed.
E-mail: okadas@kumamoto-u.ac.jp

doi: 10.1111/j.1349-7006.2012.02212.x
© 2012 Japanese Cancer Association

containing 10 mM EDTA and 0.5% Triton X. After centrifugation for 5 min at 20 000*g*, supernatant samples were treated with RNase A (Qiagen, Valencia, CA, USA) and Proteinase K (Wako Pure Chemical, Osaka, Japan). Subsequently, 20 μL of 5 M NaCl and 120 μL isopropanol were added to the sample and kept at −20°C for 6 h. Following centrifugation for 15 min at 20 000*g*, the pellets were dissolved in 20 μL TE buffer (10 mM Tris–HCl and 1 mM EDTA) as loading samples. To assess the DNA fragmentation pattern, samples were loaded onto 1.5% agarose gel and electrophoretically separated.

Western blot analysis. For whole cell extraction, BCBL-1 cells treated with 100 μM berberine for 0, 1, 3 and 6 h were collected and washed in cold PBS before the addition of 100 μL cold lysis buffer (25 mM HEPES, 10 mM $Na_4P_2O_7 \cdot 10H_2O$, 100 mM NaF, 5 mM EDTA, 2 mM Na_3VO_4 and 1% Triton X-100). After rotation for 2 h at 4°C, whole cell extracts were obtained by centrifugation at 20 000*g* for 15 min. For nuclear extraction, BCBL-1 cells treated with 100 μM berberine for 0, 1, 3 and 6 h were collected and washed in cold PBS before the addition of 400 μL cold buffer A (10 mM HEPES-KOH pH 7.9, 1.5 mM $MgCl_2$, 10 mM KCl, 0.1% NP-40, 0.5 mM DTT, 0.5 mM PMSF, 2 μg/mL pepstatin A, 2 μg/mL aprotinin and 2 μg/mL leupeptin). After incubation on ice for 10 min, the samples were vortexed for 10 sec. Nuclei were pelleted by centrifugation at 2000*g* for 1 min and washed once with buffer A. Then, 50 μL of buffer C (50 mM HEPES-KOH pH 7.9, 10% glycerol, 420 mM KCl, 5 mM $MgCl_2$, 0.1 mM EDTA, 1 mM DTT, 0.5 mM PMSF, 2 μg/mL pepstatin A, 2 μg/mL aprotinin and 2 μg/mL leupeptin) was added to the nuclei, before incubating on ice for 30 min. Nuclear extracts were obtained by centrifugation at 20 000*g* for 15 min. Whole or nuclear extracts (40 μg protein) were separated by 10% SDS-PAGE and blotted onto a PVDF membrane (GE Healthcare, Tokyo, Japan). Detection was performed using the Enhanced Chemiluminescence Western Blotting Detection System (ECL; GE Healthcare Bio-Science, Buckinghamshire, UK).

Primary antibodies were as follows: anti-cleaved caspase-3 (9661), anti-caspase 9 (9502), anti-phospho (Ser180/181)-IKKα/β (2681), anti-phospho (Ser32/36)-IκBα (9246), anti-p65 (536) (Cell Signaling Technology, Danvers, MA, USA), anti-IKKα/β (H-470), anti-IκBα (C-21) and anti-γ tublin (C-20) (Santa Cruz Biotechnology, Santa Cruz, CA, USA), anti-Hsc70 (SPA-815) (Stressgen Bioreagents, Ann Arbor, MI, USA).

Electrophonic mobility shift assay. An EMSA was performed using a second generation DIG Gel Shit Kit (Roche Diagnostics, Mannheim, Germany). Briefly, double-stranded oligonucleotide probes containing the immunoglobulin kappa (Igκ) light chain NF-κB site and the Oct-1 binding site were purchased from Promega (Madison, WI). The oligonucleotide was 3′ end-labeled with a digoxigenin-11-ddUTP. The nuclear extract (10 μg protein) from BCBL-1 cells was incubated with 1 μg poly[d(I-C)], 0.1 μg poly-L lysine and DIG-labeled oligonucleotide in binding buffer (20 mM HEPES pH 7.6, 1 mM EDTA, 10 mM $(NH_4)_2SO_4$, 0.2% Tween20 and 30 mM KCl) for 15 min at 25°C. After incubation, 5× loading buffer (0.25× TBE and 60% glycerol) was added, and the samples were separated on 6% acrylamide gel in 0.5× TBE buffer. The oligonucleotide was electroblotted onto a positively charged nylon membrane (Roche Diagnostics) and immunodetected using anti-digoxigenin-AP.

Xenograft mouse model. NOD Rag-2-deficient ($Rag\text{-}2^{-/-}$) mice and NOD Jak3-deficient ($Jak3^{-/-}$) mice were established by crossing $Rag\text{-}2^{-/-}$ mice or $Jak3^{-/-}$ mice with the NOD strain for 10 generations, respectively. NOD Rag-2/Jak3 double-deficient ($Rag\text{-}2^{-/-}Jak3^{-/-}$) mice (NRJ mice) were established by crossing NOD $Rag\text{-}2^{-/-}$ mice and NOD $Jak3^{-/-}$ mice, and were housed and monitored in our animal research facility according to institutional guidelines. All experimental procedures and protocols were approved by the Institutional Animal Care and Use Committee at Kumamoto University. Twelve week-old NRJ male mice were inoculated i.p. with 7×10^6 BCBL-1 cells suspended in 200 μL PBS. The mice were then treated with i.p. injections of PBS or berberine (10 mg/kg, three times a week). Tumor burden was evaluated by measuring the body weight and volume of ascites. For assessment of overall survival, Kaplan–Meier analysis was performed and *P*-values were determined by two-tailed analysis using the log-rank test.

Immunohistochemistry. To investigate the expression of KSHV/HHV-8 ORF73 (LANA) protein, tissue samples were fixed with 10% neutral-buffered formalin, embedded in paraffin and cut into 4-μm sections. The sections were deparaffinized by sequential immersion in xylene and ethanol, and rehydrated in distilled water. They were then irradiated for 15 min in a microwave oven for antigen retrieval. Endogenous peroxidase activity was blocked by immersing the sections in methanol/0.6% H_2O_2 for 30 min at room temperature. Affinity-purified PA1-73N antibody,[29] diluted 1:3000 in PBS/5% BSA, was then applied, and the sections were incubated

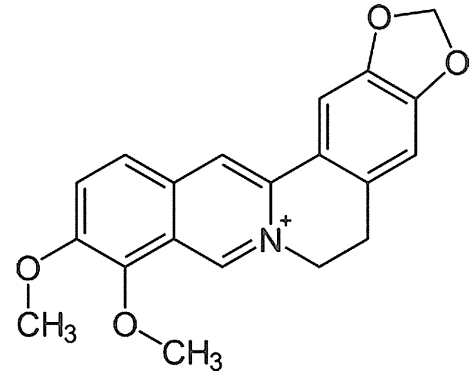

Fig. 1. Chemical structure of berberine chloride.

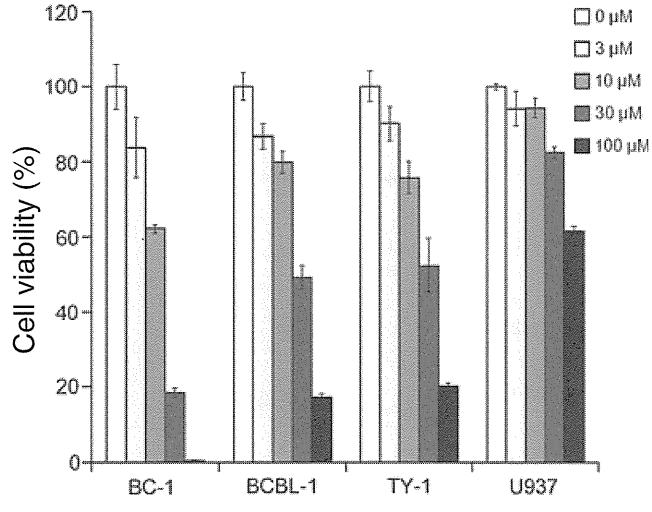

Fig. 2. Berberine inhibits the proliferation of primary effusion lymphoma (PEL) cells. PEL cell lines (BC-1, BCBL-1 and TY-1) and non-PEL cell line (U937) were incubated with 0, 3, 10, 30, 10 and 100 μM berberine for 24 h. A cell proliferation assay was carried out using MTT as described in the Materials and Methods. One representative result from three independent experiments is shown.

doi: 10.1111/j.1349-7006.2012.02212.x
© 2012 Japanese Cancer Association

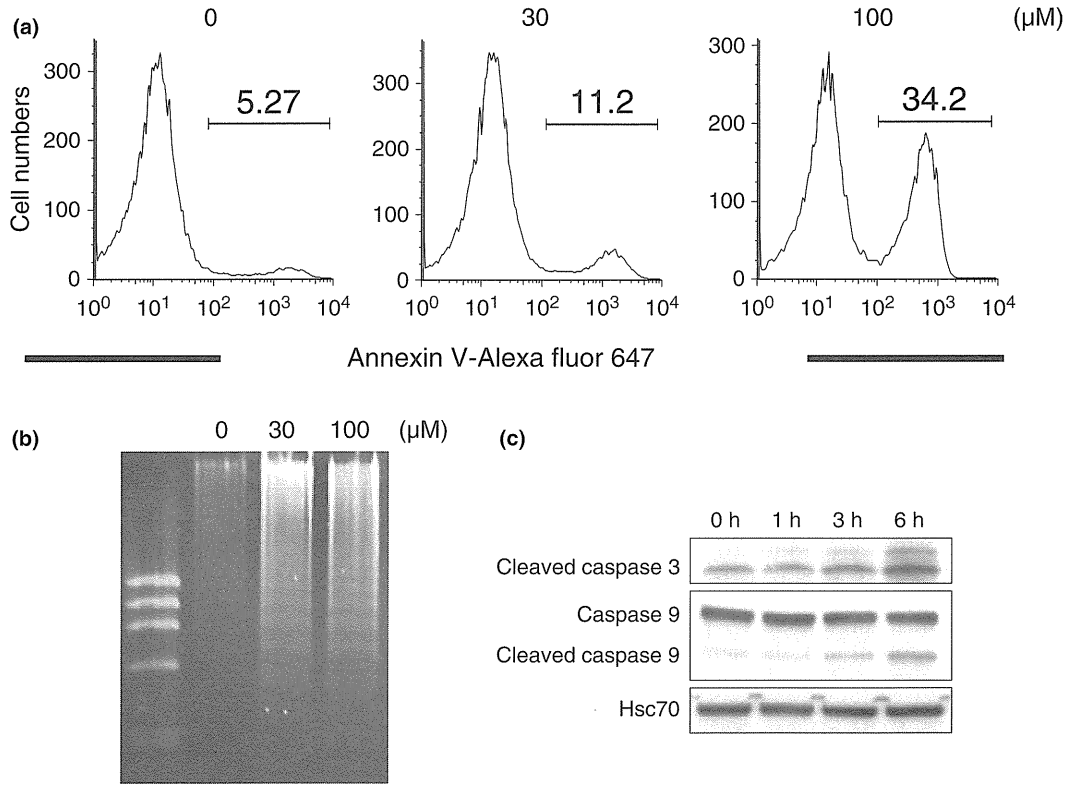

Fig. 3. Berberine induces apoptosis in BCBL-1 cells. (a) Berberine-induced apoptosis was detected by Annexin V staining. A primary effusion lymphoma cell line, BCBL-1, was treated with berberine (30, 100 μM) for 24 h and was subsequently stained with Annexin V-Alexa fluor 647 before being analyzed by flow cytometry. (b) Berberine caused DNA fragmentation of nuclei. BCBL-1 cells were treated with berberine (30, 100 μM) for 48 h. (c) BCBL-1 cells were treated with 100 μM berberine for 0, 1, 3 and 6 h and total proteins were extracted for western blotting.

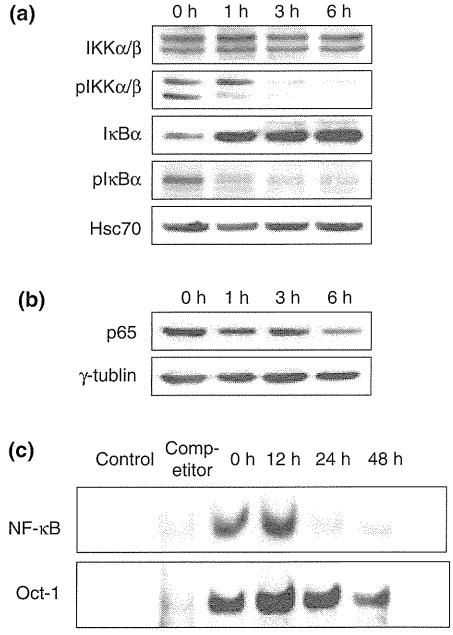

Fig. 4. Inhibitory effects of berberine on the expression of NF-κB pathways. (a) A primary effusion lymphoma cell line, BCBL-1, was treated with 100 μM berberine for 0, 1, 3 and 6 h and total proteins were extracted for western blotting. (b) BCBL-1 cells were treated with 100 μM berberine for 0, 1, 3 and 6 h and nuclear proteins were extracted for western blotting to detect NF-κB p65. (c) BCBL-1 cells were treated with 100 μM berberine for 0, 12, 24 and 48 h and assessed for NF-κB DNA binding activity by EMSA using an NF-κB-specific oligonucleotide probe.

overnight at 4°C. After washing in PBS twice, the second and third reactions and the amplification procedure were performed using kits according to the manufacturer's instructions (Catalyzed Signal Amplification System; DAKO, Copenhagen, Denmark). The signal was visualized using 0.2 mg/mL diaminobenzidine and 0.015% H_2O_2 in 0.05 M Tris–HCl, pH 7.6.

RT-PCR. Total RNA was extracted from the cells using Trizol (Invitrogen, Carlsbad, CA, USA). First-strand cDNA was synthesized from RNA using a PrimeScript RT-PCR kit (Takara Bio, Otsu, Japan) with random primers. The PCR products were analyzed by 1.5% agarose gel electrophoresis and ethidiumbromide staining. Primer sequences were as follows:

ORFK13(v-FLIP): 5′-ATTGACATTAGGGCATCC-3′ and 5′-AAAGGAGGAGGGCAGGTT-3′,[30] ORF73(LANA): 5′-GAAGTGGATTACCCTGTTGTTAGC-3′ and 5′-TTGGATCT-CGTCTTCCATCC-3′,[30] mouse G3PDH: 5-TGAAGGTCGGT-GTGAACGGATTTGGC-3′ and 5′-CATGTAGGCCATGAGG-TCCACCAC-3′.[31]

Statistical analysis. Data are expressed as the mean ± SD. The statistical significance of the differences observed between experimental groups was determined using Student's *t*-test, and $P < 0.05$ was considered significant.

Results

Berberine inhibits proliferation and induces apoptosis in primary effusion lymphoma cells. The chemical structure of berberine is shown in Figure 1 and has a molecular weight of 371.8. We first determined whether treatment with berberine leads to the inhibition of PEL cell proliferation using MTT assay. Three PEL cell lines (BC-1, BCBL-1 and TY-1) were cultured with varying concentrations of berberine (0, 3, 10, 30

© 2012 Japanese Cancer Association

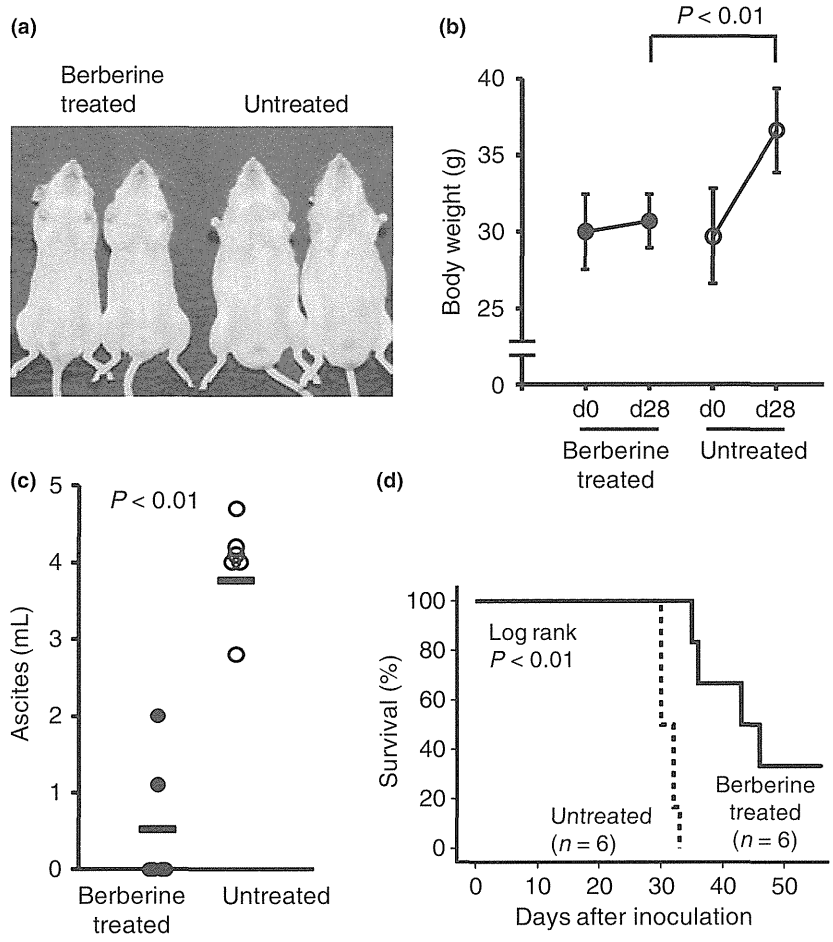

Fig. 5. Treatment of NOD/Rag-2/Jak-3-deficient mice with berberine suppresses the development of PEL *in vivo*. (a) Photograph of berberine-treated and untreated ascites-bearing mice 4 weeks after inoculation with BCBL-1 i.p. (b) The body weight of mice 4 weeks after inoculation with BCBL-1 cells in berberine-treated or untreated mice is shown as the mean ± SD of 6 mice. (c) The volume of ascites 4 weeks after inoculation with BCBL-1 cells in mice is shown as the mean ± SD of 6 mice. (d) Overall survival curve. Treatment with berberine prolongs survival *in vivo*.

and 100 μM) for 24 h, and proliferation was analyzed by MTT assay. Figure 2 shows that as the dose of berberine increased from 3 to 100 μM, cell growth inhibition increased in a dose-dependent fashion in all PEL cell lines. The IC50 (50% inhibitory concentration) for BC-1, BCBL-1 and TY-1 were 13.56, 29.17 and 32.82 μM. In contrast, the IC50 value is >100 μM for non-PEL cell line, U937. In subsequent experiments, we determined whether the observed suppressive effects of berberine in MTT assay were due to the induction of apoptosis. We used Annexin V staining and DNA ladder formation to detect apoptosis. As shown in Figure 3(a), 30 and 100 μM berberine treatment for 24 h caused apoptosis in BCBL-1. As shown in Figure 3(b), berberine treatment for 48 h caused DNA fragmentation, which is a characteristic of apoptosis cell death. Next, we analyzed cleaved caspase 3 and cleaved caspase 9 to further confirm that berberine induced apoptosis in PEL cells. As shown in Figure 3(c), berberine treatment of BCBL-1 induced time-dependent cleavage of caspase 3 and caspase 9, hallmarks of cells undergoing apoptosis, in western blotting.

Berberine suppresses NF-κB activity in PEL cells. It was reported previously that NF-κB was required for the survival and proliferation of PEL cells.[4,32,33] Because NF-κB is constitutively active in PEL cells,[34] we examined whether berberine inhibited NF-κB activation. BCBL-1 constitutively expressed both total and phosphorylated IKK and IκB, upstream of NF-κB. When BCBL-1 was treated with 100 μM berberine for 0, 1, 3 and 6 h, berberine treatment reduced phosphorylated IKK and phosphorylated IκB, whereas total IκB was increased (Fig. 4a), suggesting that inhibition of IKK phosphorylation leads to the accumulation of IκB by blocking the phosphorylation and degradation of IκB protein. Next, we fractioned nuclear protein and analyzed the expression of p65 by western blotting (Fig. 4b) to confirm p65 NF-κB suppression by berberine. When PEL cell lines were treated with 100 μM berberine for 6 h, the amount of nuclear p65 NF-κB protein was reduced, indicating that berberine suppresses NF-κB activity. Thus, berberine mainly suppresses p65 NF-κB nuclear translocation by inhibiting the upstream of NF-κB. To confirm that berberine could inhibit NF-κB activity in PEL cells, we performed EMSA with DIG-labeled double-stranded NF-κB oligonucleotides. Berberine also suppresses constitutive NF-κB binding activity for 24 and 48 h (Fig. 4c). These results demonstrate that berberine inhibits the constitutive NF-κB activity of PEL cells.

***In vivo* effect of berberine in severe immunodeficient mice inoculated i.p. with BCBL-1.** As the *in vitro* results suggest that berberine could be an effective treatment against PEL, we assessed the *in vivo* effects of berberine in the immunodeficient mouse model. Severe immunodeficient, NRJ mice were

doi: 10.1111/j.1349-7006.2012.02212.x
© 2012 Japanese Cancer Association

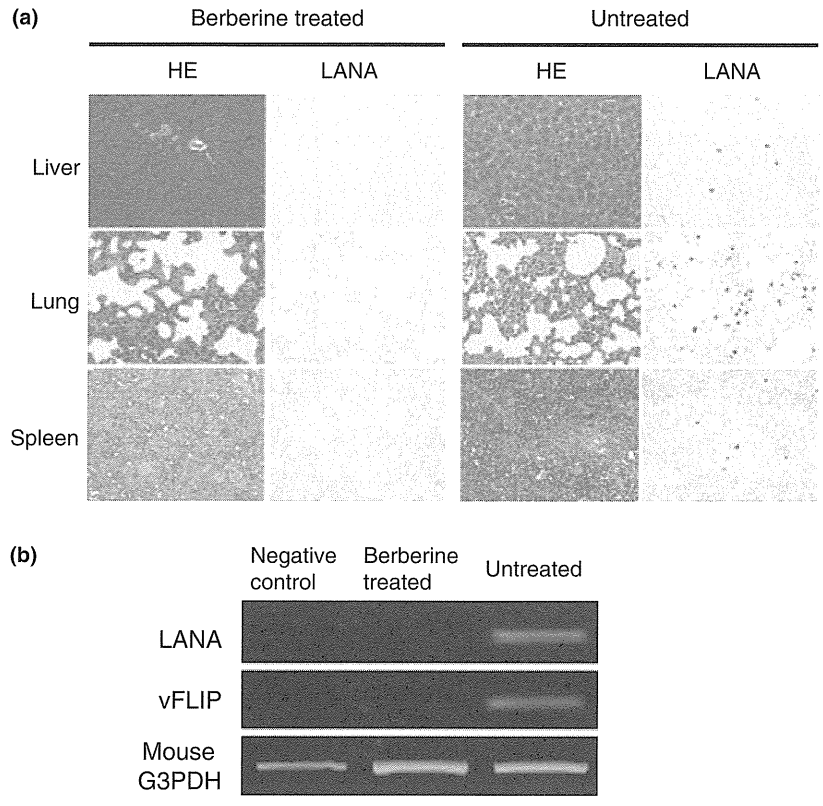

Fig. 6. Invasion of primary effusion lymphoma cells into the organs of BCBL-1-inoculated mice on day 28. (a) Hematoxylin–eosin (HE) staining and immunohistochemical staining using anti-LANA (PA1-73N antibody) was performed to detect BCBL-1 in the liver, lung and spleen. (b) Viral gene expression after treatment with berberine. Viral gene expression in spleen of berberine treated and untreated mouse was examined by RT-PCR. A representative result from two experiments is shown.

inoculated i.p. with 7×10^6 BCBL-1 cells. BCBL-1 produced profuse ascites within 4 weeks of inoculation (Fig. 5a). As patients with PEL show lymphomatous effusion in body cavities without a definable tumor mass,[2,35] these mice could be clinically equivalent to the PEL model. A dose of 10 mg/kg berberine or PBS alone was administrated via i.p. injection on day 3 after cell inoculation, and then three times a week. The 50% lethal dose of berberine from i.p. injections has already been reported and is 57.6103 mg/kg.[36] Hence, the dosage of berberine *in vivo* in our experiment was expected to be safe. Berberine-treated mice appeared to stay healthy, and the body weight did not change, whereas the body weight of untreated mice significantly increased compared to that of berberine-treated mice on day 28 (36.6 ± 2.7 g *vs* 30.7 ± 1.7 g, $n = 6$, $P < 0.01$; Fig. 5b). Moreover, the volume of ascites was significantly lower than in untreated mice on day 28 (3.8 ± 0.6 mL *vs* 0.5 ± 0.8 mL, $n = 6$, $P < 0.01$; Fig. 5c). As shown in Figure 5d, treatment with berberine significantly prolonged survival of the mice (log-rank test, $P < 0.01$). These results indicate that treatment with berberine delays or inhibits the growth of PEL cells and produces a survival benefit.

Organ invasion by PEL cells on day 28 was evaluated by hematoxylin–eosin staining and LANA immunostaining. We found that mice inoculated i.p. with BCBL-1 exhibited invasion into the liver, lung and spleen without macroscopic lymphoma formation (Fig. 6a). The number of LANA-positive cells in berberine-treated mice was significantly reduced (0–1 cells per field magnification, ×40) compared to untreated mice (10–20 cells per field magnification, ×40). The mRNA expression levels of vFLIP and LANA were downregulated in the spleen of berberine-treated mouse (Fig. 6b). These data demonstrated that berberine significantly inhibits the growth and infiltration of PEL cells *in vivo* and could be a potentially therapeutic agent in patients with PEL.

Discussion

The clinical course of PEL is very aggressive and generally refractory to conventional chemotherapy; hence, novel therapeutic strategies such us molecular targeting therapy are needed. In the present study, we investigated the antitumor effects of a naturally occurring isoquinoline alkaloid, berberine, on PEL cells both *in vitro* and *in vivo*, and showed that berberine inhibited the NF-κB pathway with the suppression of IKK phosphorylation, IκB phosphorylation and IκB degradation. In KSHV/HHV-8-infected cells, vFLIP, a homologue of cellular FLIP protein, has the ability to activate the NF-κB pathway by binding to the IKK complex.[33,37,38] Moreover, inhibition of NF-κB activity leads to the apoptosis of KSHV-infected PEL cells.[4,32] These results suggest that inhibition of NF-κB is an effective target for the treatment of PEL. Activation of NF-κB is involved in various kinds of cancer development and progression,[39,40] indicating that NF-κB is a good molecular target for cancer treatment.

Berberine has long been used as a stomachic, an antidiarrheal agent, an antibiotic and an anti-inflammatory in Asian countries and has been shown to have few side effects.[8,9,13] Berberine has been reported to have various pharmacological effects, including an arresting effect on cell cycle progress, inhibition of tumor cell proliferation and the induction of apoptosis, and the mechanism of antitumor activity differs among cell lines.[14–17,41,42] Several reports have demonstrated that berberine inhibits cancer cell migration by suppressing COX-2, MMP-2, MMP-9 and urokinase-plasminogen

© 2012 Japanese Cancer Association

activator,[19–21] downstream molecules of NF-κB. We showed here that berberine induced the apoptosis of PEL by inhibiting IKK phosphorylation, the upstream target of the NF-κB pathway. Consequently, berberine abrogates the phosphorylation of IκB (Fig. 4a), NF-κB nuclear translocation (Fig. 4b) and DNA binding activity (Fig. 4c). Previously, we reported biscoclaurine alkaloid cepharanthine-induced apoptosis of PEL cells mainly via inhibiting p65 activation. In this study, berberine inhibits IKK activation, the upstream of the NF-κB pathway, and causes efficient apoptosis of PEL cells. Inhibiting IKK activation is also considered to be a rational pharmacologic target because vFLIP activates IKK in PEL cells.

We also confirmed the therapeutic effect of berberine against PEL in a xenograft mouse model. We used NRJ mice, which displayed rapid and efficient engraftment of PEL cells, as a small animal system. NRJ mice display not only complete deficiency in mature T/B lymphocytes and complement protein but also complete deficiency of NK cells, such as in NOD/Scid/common γ-deficient (NOG) mice[43,44] and NOD/Scid/Jak3-deficient (NOJ) mice,[45] and provide the ideal microenvironment for the propagation and increase of PEL cells. Although both scid and Rag mutations prevent the recombination of genes required for functional B and T cell receptors, the Prkdc gene disrupted by the scid mutation is expressed broadly and is involved in DNA repair, while expression of rag genes is limited to hematopoietic cells and is involved only in the DNA recombination of T and B cell receptor genes. Thus, scid mice are more sensitive to radiation-induced or drug-induced DNA damage than their Rag mutation counterparts. In addition, the scid mutation is known to show a leaky phenomenon in which functional T and B cells are produced with aging and ionized irradiation.[46] Taken together, NRJ mice are expected to be more convenient recipients of human cell xeno-transplantation.

The formation of malignant ascites without solid lymphoma formation displayed in PEL xenograft NRJ mice reflects the clinical nature of human PEL and they could be a quite useful *in vivo* model for studying PEL and HHV-8 pathogenesis. Berberine has been reported to suppress tumor invasion[21] and phorbol-ester-induced tumor promotion,[22] chemical-induced carcinogenesis[23] *in vivo*; however, the direct antitumor effect and doses of berberine used in animal studies are unclear. In this study, we observed that administration of 10 mg/kg berberine three times a week showed significant reduction of ascites and tumor invasion with no apparent adverse effects on NRJ mice (Figs 5,6). Tumor invasion is related to some target genes of NF-κB, such as MMP and vascular endothelial growth factor.[39] We confirmed that suppressing NF-κB was also effective for invasion of PEL cells *in vivo*. Further studies in animals suggest a new direction in the treatment of refractory malignancies such as PEL.

The effects of berberine on PEL cells other than the NF-κB pathway are expected because berberine also affects NF-κB-independent tumors and exerts diverse pharmacological effects.[9,13,15] Elucidating the pharmacological diversity of berberine could lead to the development of novel effective therapies for a variety of malignancies as well as PEL. Berberine has been reported to have antiretroviral activity against HIV[47] and to reduce endoplasmic reticulum stress by preventing an HIV protease inhibitor-induced inflammatory response.[48] In AIDS patients who develop PEL, concomitant treatment with berberine could contribute to not only antitumor and tumor-preventing activities, but also antiretroviral therapy.

In conclusion, our data have shown the ability of berberine to induce cell death by blocking the NF-κB pathway in PEL cells.

Acknowledgments

We thank Ms I. Suzu for technical assistance and Ms K. Tokunaga for secretarial assistance. This work was supported in part by a Health and Labour Sciences Research Grant from the Ministry of Health, Labour, and Welfare of Japan (H22-AIDS-I-002), and by the Global Center of Excellence program "Global Education and Research Center Aiming at the Control of AIDS," and Grants-in-Aid for Science Research (Nos. 21107522 and 21591209) from the Ministry of Education, Science, Sports, and Culture of Japan.

Disclosure Statement

The authors have no conflicts of interest to declare.

References

1 Ansari MQ, Dawson DB, Nador R *et al.* Primary body cavity-based AIDS-related lymphomas. *Am J Clin Pathol* 1996; **105**: 221–9.
2 Nador RG, Cesarman E, Chadburn A *et al.* Primary effusion lymphoma: a distinct clinicopathologic entity associated with the Kaposi's sarcoma-associated herpes virus. *Blood* 1996; **88**: 645–56.
3 Cesarman E, Chang Y, Moore PS, Said JW, Knowles DM. Kaposi's sarcoma-associated herpesvirus-like DNA sequences in AIDS-related body-cavity-based lymphomas. *N Engl J Med* 1995; **332**: 1186–91.
4 Keller SA, Schattner EJ, Cesarman E. Inhibition of NF-kappaB induces apoptosis of KSHV-infected primary effusion lymphoma cells. *Blood* 2000; **96**: 2537–42.
5 Aoki Y, Feldman GM, Tosato G. Inhibition of STAT3 signaling induces apoptosis and decreases survivin expression in primary effusion lymphoma. *Blood* 2003; **101**: 1535–42.
6 Uddin S, Hussain AR, Al-Hussein KA *et al.* Inhibition of phosphatidylinositol 3′-kinase/AKT signaling promotes apoptosis of primary effusion lymphoma cells. *Clin Cancer Res* 2005; **11**: 3102–8.
7 Takahashi-Makise N, Suzu S, Hiyoshi M *et al.* Biscoclaurine alkaloid cepharanthine inhibits the growth of primary effusion lymphoma in vitro and in vivo and induces apoptosis via suppression of the NF-kappaB pathway. *Int J Cancer* 2009; **125**: 1464–72.
8 Grycova L, Dostal J, Marek R. Quaternary protoberberine alkaloids. *Phytochemistry* 2007; **68**: 150–75.
9 Tang J, Feng Y, Tsao S, Wang N, Curtain R, Wang Y. Berberine and Coptidis rhizoma as novel antineoplastic agents: a review of traditional use and biomedical investigations. *J Ethnopharmacol* 2009; **126**: 5–17.
10 Lau CW, Yao XQ, Chen ZY, Ko WH, Huang Y. Cardiovascular actions of berberine. *Cardiovasc Drug Rev* 2001; **19**: 234–44.
11 Kong W, Wei J, Abidi P *et al.* Berberine is a novel cholesterol-lowering drug working through a unique mechanism distinct from statins. *Nat Med* 2004; **10**: 1344–51.
12 Kuo CL, Chi CW, Liu TY. The anti-inflammatory potential of berberine in vitro and in vivo. *Cancer Lett* 2004; **203**: 127–37.
13 Imanshahidi M, Hosseinzadeh H. Pharmacological and therapeutic effects of Berberis vulgaris and its active constituent, berberine. *Phytother Res* 2008; **22**: 999–1012.
14 Letasiova S, Jantova S, Cipak L, Muckova M. Berberine-antiproliferative activity in vitro and induction of apoptosis/necrosis of the U937 and B16 cells. *Cancer Lett* 2006; **239**: 254–62.
15 Hwang JM, Kuo HC, Tseng TH, Liu JY, Chu CY. Berberine induces apoptosis through a mitochondria/caspases pathway in human hepatoma cells. *Arch Toxicol* 2006; **80**: 62–73.
16 Mantena SK, Sharma SD, Katiyar SK. Berberine, a natural product, induces G1-phase cell cycle arrest and caspase-3-dependent apoptosis in human prostate carcinoma cells. *Mol Cancer Ther* 2006; **5**: 296–308.
17 Lin JP, Yang JS, Lee JH, Hsieh WT, Chung JG. Berberine induces cell cycle arrest and apoptosis in human gastric carcinoma SNU-5 cell line. *World J Gastroenterol* 2006; **12**: 21–8.
18 Pandey MK, Sung B, Kunnumakkara AB, Sethi G, Chaturvedi MM, Aggarwal BB. Berberine modifies cysteine 179 of IkappaBalpha kinase, suppresses nuclear factor-kappaB-regulated antiapoptotic gene products, and potentiates apoptosis. *Cancer Res* 2008; **68**: 5370–9.
19 Singh T, Vaid M, Katiyar N, Sharma S, Katiyar SK. Berberine, an isoquinoline alkaloid, inhibits melanoma cancer cell migration by reducing the

doi: 10.1111/j.1349-7006.2012.02212.x
© 2012 Japanese Cancer Association

expressions of cyclooxygenase-2, prostaglandin E and prostaglandin E receptors. *Carcinogenesis* 2011; **32**: 86–92.
20 Ho YT, Yang JS, Li TC *et al.* Berberine suppresses in vitro migration and invasion of human SCC-4 tongue squamous cancer cells through the inhibitions of FAK, IKK, NF-kappaB, u-PA and MMP-2 and -9. *Cancer Lett* 2009; **279**: 155–62.
21 Peng PL, Hsieh YS, Wang CJ, Hsu JL, Chou FP. Inhibitory effect of berberine on the invasion of human lung cancer cells via decreased productions of urokinase-plasminogen activator and matrix metalloproteinase-2. *Toxicol Appl Pharmacol* 2006; **214**: 8–15.
22 Nishino H, Kitagawa K, Fujiki H, Iwashima A. Berberine sulfate inhibits tumor-promoting activity of teleocidin in two-stage carcinogenesis on mouse skin. *Oncology* 1986; **43**: 131–4.
23 Anis KV, Rajeshkumar NV, Kuttan R. Inhibition of chemical carcinogenesis by berberine in rats and mice. *J Pharm Pharmacol* 2001; **53**: 763–8.
24 Cesarman E, Moore PS, Rao PH, Inghirami G, Knowles DM, Chang Y. In vitro establishment and characterization of two acquired immunodeficiency syndrome-related lymphoma cell lines (BC-1 and BC-2) containing Kaposi's sarcoma-associated herpesvirus-like (KSHV) DNA sequences. *Blood* 1995; **86**: 2708–14.
25 Renne R, Zhong W, Herndier B *et al.* Lytic growth of Kaposi's sarcoma-associated herpesvirus (human herpesvirus 8) in culture. *Nat Med* 1996; **2**: 342–6.
26 Katano H, Hoshino Y, Morishita Y *et al.* Establishing and characterizing a CD30-positive cell line harboring HHV-8 from a primary effusion lymphoma. *J Med Virol* 1999; **58**: 394–401.
27 Sundstrom C, Nilsson K. Establishment and characterization of a human histiocytic lymphoma cell line (U-937). *Int J Cancer* 1976; **17**: 565–77.
28 Sellins KS, Cohen JJ. Gene induction by gamma-irradiation leads to DNA fragmentation in lymphocytes. *J Immunol* 1987; **139**: 3199–206.
29 Katano H, Sato Y, Kurata T, Mori S, Sata T. High expression of HHV-8-encoded ORF73 protein in spindle-shaped cells of Kaposi's sarcoma. *Am J Pathol* 1999; **155**: 47–52.
30 Krishnan HH, Naranatt PP, Smith MS, Zeng L, Bloomer C, Chandran B. Concurrent expression of latent and a limited number of lytic genes with immune modulation and antiapoptotic function by Kaposi's sarcoma-associated herpesvirus early during infection of primary endothelial and fibroblast cells and subsequent decline of lytic gene expression. *J Virol* 2004; **78**: 3601–20.
31 Yamamoto H, Hatano M, Iitsuka Y, Mahyar NS, Yamamoto M, Tokuhisa T. Two forms of Hox11 a T cell leukemia oncogene, are expressed in fetal spleen but not in primary lymphocytes. *Mol Immunol* 1995; **32**: 1177–82.
32 Keller SA, Hernandez-Hopkins D, Vider J *et al.* NF-kappaB is essential for the progression of KSHV- and EBV-infected lymphomas in vivo. *Blood* 2006; **107**: 3295–302.
33 Guasparri I, Keller SA, Cesarman E. KSHV vFLIP is essential for the survival of infected lymphoma cells. *J Exp Med* 2004; **199**: 993–1003.
34 Jost PJ, Ruland J. Aberrant NF-kappaB signaling in lymphoma: mechanisms, consequences, and therapeutic implications. *Blood* 2007; **109**: 2700–7.
35 Chen YB, Rahemtullah A, Hochberg E. Primary effusion lymphoma. *Oncologist* 2007; **12**: 569–76.
36 Kheir MM, Wang Y, Hua L *et al.* Acute toxicity of berberine and its correlation with the blood concentration in mice. *Food Chem Toxicol* 2010; **48**: 1105–10.
37 Sun Q, Matta H, Chaudhary PM. The human herpes virus 8-encoded viral FLICE inhibitory protein protects against growth factor withdrawal-induced apoptosis via NF-kappa B activation. *Blood* 2003; **101**: 1956–61.
38 Sun Q, Zachariah S, Chaudhary PM. The human herpes virus 8-encoded viral FLICE-inhibitory protein induces cellular transformation via NF-kappaB activation. *J Biol Chem* 2003; **278**: 52437–45.
39 Karin M, Greten FR. NF-kappaB: linking inflammation and immunity to cancer development and progression. *Nat Rev Immunol* 2005; **5**: 749–59.
40 Kim HJ, Hawke N, Baldwin AS. NF-kappaB and IKK as therapeutic targets in cancer. *Cell Death Differ* 2006; **13**: 738–47.
41 Lin CC, Lin SY, Chung JG, Lin JP, Chen GW, Kao ST. Down-regulation of cyclin B1 and up-regulation of Wee1 by berberine promotes entry of leukemia cells into the G2/M-phase of the cell cycle. *Anticancer Res* 2006; **26**: 1097–104.
42 Kuo CL, Chi CW, Liu TY. Modulation of apoptosis by berberine through inhibition of cyclooxygenase-2 and Mcl-1 expression in oral cancer cells. *In Vivo* 2005; **19**: 247–52.
43 Ito M, Hiramatsu H, Kobayashi K *et al.* NOD/SCID/gamma(c)(null) mouse: an excellent recipient mouse model for engraftment of human cells. *Blood* 2002; **100**: 3175–82.
44 Shultz LD, Lyons BL, Burzenski LM *et al.* Human lymphoid and myeloid cell development in NOD/LtSz-scid IL2R gamma null mice engrafted with mobilized human hemopoietic stem cells. *J Immunol* 2005; **174**: 6477–89.
45 Okada S, Harada H, Ito T, Saito T, Suzu S. Early development of human hematopoietic and acquired immune systems in new born NOD/Scid/Jak3null mice intrahepatic engrafted with cord blood-derived CD34 + cells. *Int J Hematol* 2008; **88**: 476–82.
46 Bosma GC, Fried M, Custer RP, Carroll A, Gibson DM, Bosma MJ. Evidence of functional lymphocytes in some (leaky) scid mice. *J Exp Med* 1988; **167**: 1016–33.
47 Bodiwala HS, Sabde S, Mitra D, Bhutani KK, Singh IP. Synthesis of 9-substituted derivatives of berberine as anti-HIV agents. *Eur J Med Chem* 2011; **46**: 1045–9.
48 Zha W, Liang G, Xiao J *et al.* Berberine inhibits HIV protease inhibitor-induced inflammatory response by modulating ER stress signaling pathways in murine macrophages. *PLoS ONE* 2010; **5**: e9069.

© 2012 Japanese Cancer Association

©2012 The Japanese Society for AIDS Research

症例報告

エファビレンツ，テノホビル/エムトリシタビンを大量服用した症例の血中濃度推移について

大石　裕樹[1,4]，安藤　仁[2]，高橋　昌明[3]，髙濱宗一郎[4]，
喜安　純一[4]，南　留美[4]，石橋　誠[1]，山本　政弘[4]

[1] 国立病院機構九州医療センター薬剤科，[2] 聖マリアンナ医科大学難病治療研究センター，
[3] 国立病院機構名古屋医療センター薬剤科，[4] 国立病院機構九州医療センター臨床研究センター

目的：エファビレンツ（EFV），テノホビル/エムトリシタビン（TDF/FTC）の大量服用後に血中濃度を経時的に測定した症例を経験したので報告する。

症例：29歳，男性。EFV（200 mg）を90錠，TDF/FTCを30錠服用し，緊急入院となった。入院後，薬用炭の投与とハイドレーションを行いながら，EFV，TDFについて経時的に血中濃度を測定した。EFVの血中濃度は，600 mgを単回投与したときのトラフ値と比較して24時間値で約8倍まで上昇し，96時間値で同等の値まで低下した。TDFの血中濃度は，300 mgを単回投与したときのトラフ値と比較して，48時間値で約12倍まで上昇し，同等の値まで減少するのに96時間を要した。検査値異常としてCK-MB値の上昇が観察された。

考察：EFVは著しい消失時間の延長は観察されず，TDFは吸収過程の遷延が観察された。EFVは薬用炭に吸着されやすく，親水性の高いTDFにはハイドレーションが有効であったと考えられる。CK-MB値の上昇は，心筋障害による可能性が高いと考えられた。

キーワード：ART，大量服用，EFV，TDF

日本エイズ学会誌 **14**：42-45，2012

緒　　言

エファビレンツ（EFV）は，非核酸系逆転写酵素阻害薬に分類される抗HIV薬である。EFVは優れた抗ウイルス効果を示し，1日1回の投与が可能で，吸収に食事の影響をうけない。またテノホビル/エムトリシタビン（TDF/FTC）は2種類の核酸系逆転写酵素阻害剤の合剤で，こちらも1日1回投与が可能である。これらの薬剤は抗HIV作用に優れることと服薬の簡便さから，さまざまなガイドラインにおいて初回治療に推奨される組合せとして設定され，Antiretroviral therapy（ART）のなかでも使用頻度の高い薬剤である。

両剤とも重篤な副作用発現は稀であるが，EFVでは抑うつ状態，うつ症状の悪化，めまい，健忘，錯乱など，精神神経系の副作用が発現しやすいことが知られている[1]。またTDF/FTCは，腎機能低下症例や大量服用でTDFによる腎障害が発現しやすくなることが知られている[2]。

今回われわれは，EFV＋TDF/FTCによるARTを継続中に大量服用した症例を経験し，大量服用後の血中薬物濃度を経時的に測定した。EFVとTDF/FTCを大量服用後に血中濃度を経時的に測定した報告は少なく，臨床上有用なデータであると考えたので報告する。

症　　例

症例：29歳，男性。体重51 kg。2009年4月，HIV感染症と診断。診断時，HIV-RNA 12,000 copies/mL，CD4+リンパ球数（CD4数）は209 cells/mm^{3}であった。CD4数の低下が顕著であったため，同年6月よりEFV＋TDF/FTCによるARTが開始となった。その他の併用薬はなかった。アドヒアランスは良好であり，HIV-RNA検出感度以下，CD4数600～700 cells/mm^{3}で推移した。2010年1月，自殺企図にて自宅でEFV（200 mg）を90錠，TDF/FTCを30錠服用後，下痢，嘔吐出現し，知人に連れられ当院を受診した。自殺企図・抗HIV薬の大量服用であることから，緊急入院となった。

薬剤の排泄促進と腎保護の目的で，大量服用から192時間までは生理食塩水によるハイドレーションを行った。白色便が続いていたため，薬剤が消化管内に残存している可能性を考え，大量服用から22時間後に薬用炭（30 g）を投与した。自殺企図の原因がEFVによる精神神経系の副作用発現であった可能性も否定できず，TDFの血中濃度が上昇することによる腎機能障害も危惧されたため，EFV，TDF/FTCによるARTの継続は困難であると判断し，代替薬として大量服用から24時間後にラルテグラビル，72時間後にアバカビル/ラミブジンを開始した。

著者連絡先：大石裕樹（〒810-8563　福岡市中央区地行浜1-8-1　独立行政法人国立病院機構九州医療センター薬剤科）

2011年6月28日受付；2011年9月30日受理

EFV の血中濃度を大量服用後，24，48，72，96，120，144，168 時間で測定したところ，それぞれの測定値は，6,860，4,090，1,960，860，510，320，180 ng/mL であった（図 1）。TDF の血中濃度は大量服用から 24，48，72，96 時間で測定し，それぞれの測定値は，310，370，40，30 ng/mL であった（図 2）。

EFV の血中濃度に影響する因子として代謝酵素 CYP2B6 の遺伝子多型（G516T）が知られており，変異型ホモ（T/T）の保有者では EFV の代謝が減弱し，野生型（G/G）の患者と比較して最高血中濃度が 2～4 倍に上昇し，消失半減期が約 2 倍となる[3]。患者の同意を得て *CYP2B6*（*G516T*）遺伝子多型の解析を行ったところ，本症例は，野生型（G/G）であり，EFV の薬物動態に遺伝子多型の影響はなかったと考えられる。遺伝子多型の解析については九州医療センター倫理審査委員会での承認を得ている（受付番号：09-56）。

また，経過観察中，TDF による腎機能の低下が危惧されたが，大量服用後 120 時間まで Scr は 0.5～0.7 mg/dL で推移した。また，大量服用後 120 時間での Ccr は 72.9 mL/min であった。本症例では腎機能の低下はなかったと考えられる。

検査値異常として一過性に CK-MB 値の上昇が観察され，CK-MB の測定値は大量服用後 19，43，67，139，187 時間で 71，110，76，32，20 U/L（基準値 10～21 U/L）であった。また，同時点での CK 値は，それぞれ 68，83，72，59，48 IU/L（基準値 62～287 IU/L）で，大きな変動はなかった。その他の検査値にも大きな変動は見られなかった。その後，有害事象は発現せず，2010 年 2 月に退院となった。

考　　察

本症例で測定された EFV の血中濃度は，600 mg を単回投与したときのトラフ値（900 ng/mL）と比較して 24 時間値で約 8 倍（6,860 ng/mL）まで上昇したが，96 時間値では 860 ng/mL まで低下した。また EFV（600 mg）服薬後の血中濃度の推移（未発表データ）と比較しても 120 時間以降の血中濃度はほぼ同等であったことから，本症例では大量服用による消失時間の著しい延長はなかったと考える。

TDF の血中濃度は，300 mg を単回投与したときのトラフ

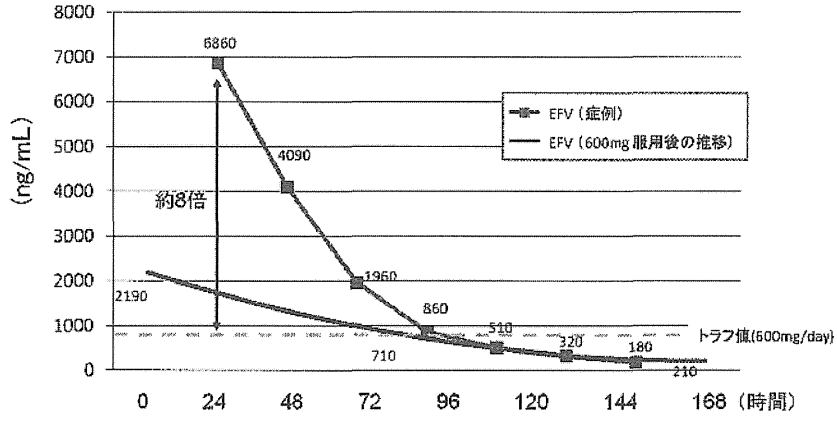

図 1　血中濃度の推移（EFV）

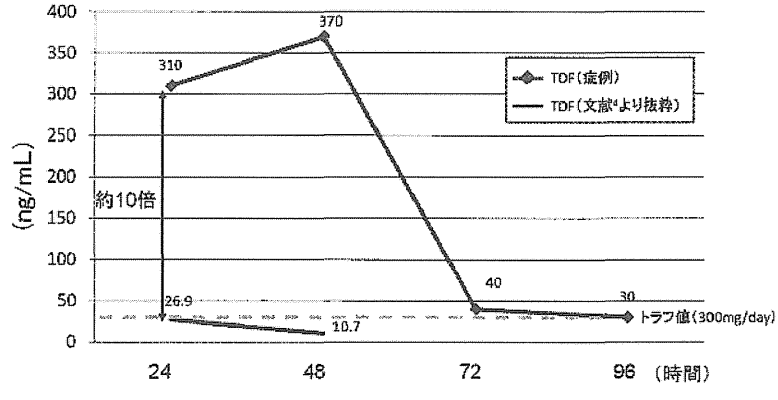

図 2　血中濃度の推移（TDF）

値（30 ng/mL）と比較して，24 時間値で約 10 倍（310 ng/mL），48 時間値では約 12 倍（370 ng/mL）まで上昇し，30 ng/mL まで減少するのに 96 時間を要した。中道[4]によって報告された TDF 300 mg 服用後の血中濃度の推移と比較しても，TDF の血中薬物動態には消失時間の延長がみられた。

EFV は脂溶性の高い薬剤で，血中でのタンパク結合率は 99.5% と高く，大部分が糞中へ排泄される[5]。そのため，透析では除去されないと考えられている。TDF は親水性が高く，大部分が尿中へ排泄され，透析によって除去される[6]。本症例では透析は行っていないが，薬剤の排泄促進と腎保護を目的としてハイドレーション，薬用炭の投与を行った。現在までにハイドレーションや薬用炭の投与が EFV，TDF の排泄を促進したという報告はないが，脂溶性の高い EFV は薬用炭によって吸着され，親水性の高い TDF の排泄はハイドレーションにより促進されると推察される。前述のとおり，本症例は大量服用から 22 時間まで白色便を呈しており，薬用炭を投与した時点では大量服用された薬剤の多くが消化管内に残存していたと考えられる。消化管内に残存した EFV が薬用炭に吸着され，吸収が抑制されたことで，EFV 消失時間の著しい延長を回避することができたと考える。また，TDF の T_{max} が約 1 時間であるにもかかわらず[6]，本症例の TDF 血中濃度は大量服用後 48 時間でピークとなった。この現象の一因として，親水性である TDF が薬用炭によって十分には除去されず，消化管に残存した TDF の吸収が遷延した可能性が考えられる。その後，TDF 血中濃度は速やかに低下しており，TDF の排泄促進という点で，ハイドレーションの有効性が示唆された。

経過観察中に一過性の上昇が観察された CK-MB 値は，主に心筋の障害で上昇する。しかしながら，現在までに EFV，TDF/FTC が副作用として心筋障害を招くという報告はなく，EFV や TDF/FTC の服用時に CK-MB 値の変動を観察した報告もない。CK-MB 値は，まれに骨格筋の障害により上昇するが，同時点での CK 値が正常範囲であったことから，本症例で観察された CK-MB 値の上昇が骨格筋由来であったとは考えにくい。したがって，大量服用後の CK-MB 値の上昇は，心筋障害によるものであった可能性が高く，EFV や TDF/FTC の大量服用が心筋障害を引き起こす可能性を示唆する。よって，EFV や TDF/FTC の大量服用時には心筋障害のモニタリングが必要ではないかと考える。

結　　語

EFV，TDF/FTC を大量服用した症例を経験し，大量服用後の血中濃度を経時的に測定した。EFV の消失時間に大きな変化は見られず，TDF の消失時間は延長した。本症例においては，薬用炭による EFV の吸収抑制と TDF の排泄促進を目的としたハイドレーションの有効性が示唆された。また EFV，TDF/FTC の大量服用に関連して心筋障害を疑う CK-MB 値の上昇が観察されたが，重篤な有害事象は観察されなかった。

文　　献

1）Haas DW, Ribaudo HJ, Kim RB, Tierney C, Wilkinson GR, Gulick RM, Clifford DB, Hulgan T, Marzolini C, Acosta EP : Pharmacogenetics of efavirenz and central nervous system side effects : An Adult AIDS Clinical Trials Group Study. AIDS 18 : 2391–2400, 2004.

2）Nelson MR, Katlama C, Montaner JS, Cooper DA, Gazzard B, Clotet B, Lazzarin A, Schewe K, Lange J, Wyatt C, Curtis S, Chen SS, Smith S, Bischofberger N, Rooney JF : The safety of tenofovir disoproxil fumarate for the treatment of HIV infection in adults : The first 4 years. AIDS 21 : 1273–1281, 2007.

3）Ribaudo HJ, Haas DW, Tierney C, Kim RB, Wilkinson GR, Gulick RM, Clifford DB, Marzolini C, Fletcher CV, Tashima KT, Kuritzkes DR, Acosta EP : Pharmacogenetics of plasma efavirenz exposure after treatment discontinuation : An Adult AIDS Clinical Trials Group Study. Clin Infect Dis 42 : 401–407, 2006.

4）中道昇：ビリアード®錠 300 mg の日本人健康成人男性を対象とした薬物動態試験．新薬と臨牀 54：941–948，2005.

5）ストックリン®錠 200 mg 医薬品インタビューフォーム（2011 年 3 月）.

6）ビリアード®錠 300 mg 医薬品インタビューフォーム（20011 年 1 月）.

The Journal of AIDS Research Vol. 14 No. 1 2012

Plasma Concentrations of Efavirenz and Tenofovir in Overdose

Yuki OHISHI[1,4], Hitoshi ANDO[2], Masaaki TAKAHASHI[3], Soichiro TAKAHAMA[4], Jyunichi KIYASU[4], Rumi MINAMI[4], Makoto ISHIBASHI[1], and Masahiro YAMAMOTO[4]

[1] Department of Pharmacy, National Hospital Organization Kyusyu Medical Center,
[2] Department of Rare Disease Research, Institute of Medical Science,
St Marianna University School of Medicine,
[3] Department of Pharmacy, National Hospital Organization Nagoya Medical Center,
[4] Department of Clinical Research Center, National Hospital Organization Kyusyu Medical Center

Case : A 29-year-old Japanese male with HIV infection had been followed up at Kyusyu Medical Center under ART with Efavirenz (EFV) and Tenofovir (TDF)/Emtricitabine. He took 18,000 mg of EFV (90 tablets) and 9,000 mg of TDF (30 tablets) with suicidal intent. At 24 h, plasma EFV concentration was 6,860 ng/mL, which was 8-fold higher compared with trough value (900 ng/mL) at single-dose administration. After 96 h, plasma EFV concentration decreased to 860 ng/mL. The elimination half-life of EFV was not prolonged in this case. In contrast, plasma TDF concentration was 310 ng/mL at 24 h and then increased to 370 ng/mL after 48 h. This value was 12-fold higher compared with trough value (30 ng/mL) at single-dose administration. After 96 h, plasma TDF concentration decreased to 30 ng/mL. This data suggests that the elimination half-life of TDF will be prolonged in overdose.

Conclusion : In this case, activated charcoal was available for adsorption of EFV. However, it was not suitable for adsorption of TDF, because TDF has a strong affinity for water. To excrete TDF from the body, an intravenous saline hydration was effective. A temporary increase of CK-MB may be caused by an injury of cardiac muscle.

Key words : ART, EFV, TDF, overdose

CASE REPORT

症例

免疫再構築症候群として発症したGraves病の1例*

古西　満　片浪雄一　忽那賢志
宇野健司　三笠桂一**

はじめに　抗HIV(human immunodeficiency virus)治療後にみられる免疫再構築症候群(immune reconstitution inflammatory syndrome：IRIS)の多くはH和見感染症である．しかし，ときには自己免疫疾患を発症することもあり，IRISは多彩な病状を呈する．

今回われわれは，サルベージ療法のため抗HIV治療を変更し，約26ヵ月後にIRISと考えるGraves病を発症した症例を経験したので報告する．

症　例

症　例：46歳，男性．
主　訴：動悸，下痢，体重減少．
家族歴：父は糖尿病，高血圧．姉は乳癌．
既往歴：1989年に慢性C型肝炎．
現病歴：血友病Aのため使用した非加熱血液製剤でHIVに感染し，1998年から抗HIV治療を開始した．仕事(長距離トラック)のため生活が不規則となり，服薬や受診が途切れがちであった．抗HIV薬の各クラスに耐性を認めたため，2004年ごろからCD4陽性細胞数が減少しはじめ，2007年7月には5/μlとなり，ニューモシスチス肺炎を発症した．ニューモシスチス肺炎の治療後9月初旬からsanilvudine(d4T)・darunavir(DRV)・ritonavir(RTV)・raltegravir(RAL)によるサルベージ療法を開始した．治療効果は良好で，HIV-RNA量は1ヵ月後には検出限界未満となり，CD4陽性細胞数も1年後には200/μl以上を維持するようになった．

その後病状は安定していたが，2009年11月中旬から食欲亢進，動悸，下痢，頻尿，体重減少が順次出現した．12月の外来受診時の検査で甲状腺機能亢進症の所見を認めたため，精査加療目的で12月下旬に入院した．

入院時身体所見：身長170 cm，体重63 kg，血圧120/78 mmHg，脈拍112/min・整，体温37.0℃．甲状腺は軽度腫大し，両側頸部に小豆大のリンパ節を数個触知した．両側膝関節の軽度変形を認めた．

入院時検査所見(Table 1)：軽度の貧血と肝機能障害を認め，CD4陽性細胞数は356/μl，HIV-RNA量は検出しなかった．TSHは低下し，FT3，FT4は増加していた．抗TPO抗体，抗TSH受容体抗体，甲状腺刺激型抗体は陽性であった．甲状腺シンチグラフィでヨード摂取率は59.4%と亢進していた．甲状腺エコーではびまん性に軽度腫大を認め，内部エコーは比較的均一であった．

臨床経過(Fig. 1)：2009年4月に行った甲状腺機能検査は正常値であったが，入院時には甲状腺機能亢進を認めた．また，抗TSH受容体抗体が陽性で，ヨード摂取率が亢進していたことから，Graves病と診断した．2008年9月の保存血清を用いて甲状腺関連の自己抗体を測定したが，すべて陰性であった．有効な抗HIV治療に変更して約26ヵ月後に発症したGraves病であり，IRISと考えた．

抗HIV治療は継続しながら，thiamazole(MMI)

---

* A Case of Graves' Disease as Immune Reconstitution Inflammatory Syndrome.
** M. Konishi(客員教授)，Y. Katanami, S. Kutsuna, K. Uno, K. Mikasa(教授)：奈良県立医科大学感染症センター．

Table 1. 入院時検査所見

末梢血		LDH	246 IU/l	HBs 抗原	(−)
WBC	5,200/μl	CK	58 IU/l	HCV 抗体	(+)
好中球	31 %	BUN	15 mg/dl	HCV-RNA	5.7 logIU/ml
好酸球	1 %	Cre	0.50 mg/dl	甲状腺関連	
リンパ球	49 %	T-cho	127 mg/dl	TSH	<0.03 μU/ml
単球	19 %	TG	172 mg/dl	FT3	19.4 pg/ml
RBC	397×10⁴/μl	Glu	99 mg/dl	FT4	6.04 ng/ml
Hb	12.8 g/dl	CRP	0.1 mg/dl	抗 Tg 抗体	≦0.3 U/ml
Ht	38.0 %	HIV 感染症関連		抗 TPO 抗体	8.5 U/ml
Plt	15.8×10⁴/μl	CD4⁺	356/μl	抗 TSH 受容体抗体	18.0 IU/l
赤沈	10 mm/1 hr	CD8⁺	796/μl	甲状腺刺激型抗体	350 %
生化学		HIV-RNA	検出せず	ヨード摂取率	59.4 %
AST	40 IU/l	肝炎ウイルス関連			
ALT	47 IU/l	HBs 抗体	(+)		

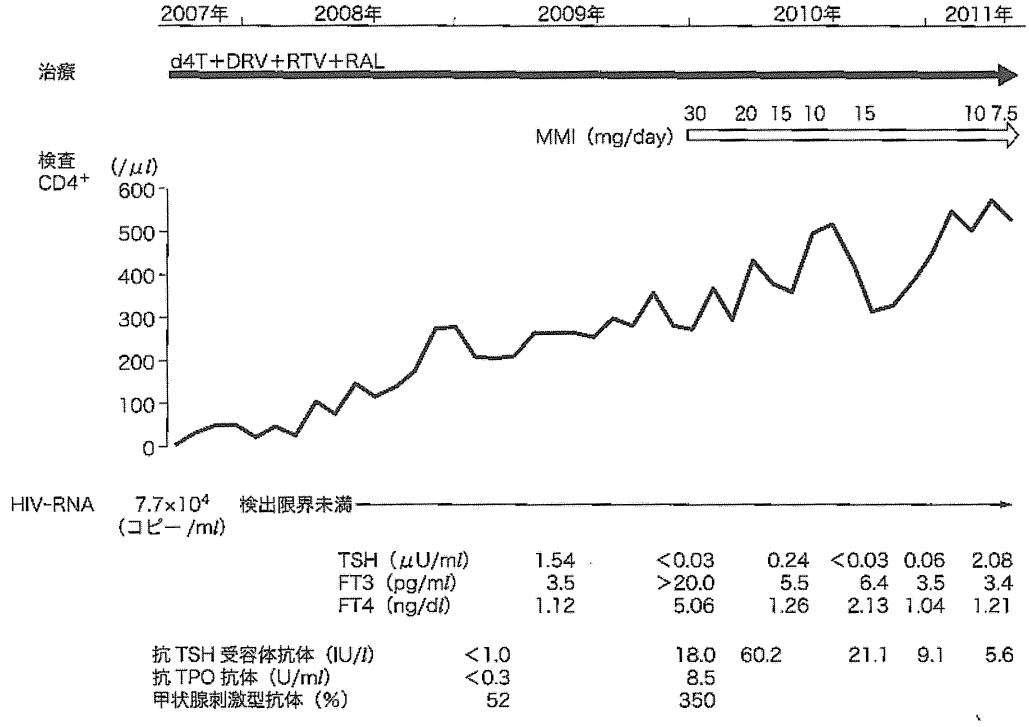

Fig. 1. 治療経過

30 mg/day の投与を開始した．約 2 週間で自覚症状は改善し，その後再発を認めていない．甲状腺機能をみながら MMI を減量し，現在は 7.5 mg/day となっている．抗 TSH 受容体抗体は MMI 投与後も 5ヵ月間は上昇したが，以後は減少し始め，2011 年 4 月には 5.6 IU/l となっている．

考　察

免疫不全が進行した症例に有効な抗 HIV 治療を開始した後に，日和見感染症などが発症，再発，

再増悪することがある[1]．これは抗 HIV 治療によって HIV 複製の抑制と免疫能の改善が起こり，体内に存在する病原体などに対する免疫応答が強く誘導されるために生じる[2]と考えられている．そのため，この現象は IRIS と呼ばれている．IRIS の発症頻度は抗 HIV 治療例の 16.1(3～39)% と報告されている[3]．その病状の多くは日和見感染症であるが[4]，ときには日和見腫瘍や自己免疫疾患を発症することもある．

われわれの経験した症例は，甲状腺中毒症を示唆する動悸などの症状，血中甲状腺ホルモン濃度の上昇，抗 TSH 受容体抗体の陽性，甲状腺シンチグラフィでのヨード摂取率亢進を認めたので，Graves 病と診断した．さらに，高度の免疫不全状態で有効な抗 HIV 治療に変更した後に CD4 陽性細胞数が増加した状況で発病していることから，IRIS として発症した Graves 病と考えた．1998 年に Gilquin ら[5]が IRIS による Graves 病の 3 症例を報告し，最近同様の報告症例が増えている[6]．わが国でも，2003 年に守谷ら[7]がはじめて症例報告し，その後学会報告が散見されるようになっている[8]．

IRIS による日和見感染症は，抗 HIV 治療の開始・変更後 3ヵ月以内に発症することが多いが，Graves 病は大半が 1 年以上経過して発症すると指摘されている[6]．本症例も抗 HIV 治療を変更して 26ヵ月後に Graves 病を発症しており，ほかの症例報告と類似している．IRIS による Graves 病がなぜ抗 HIV 治療開始後 1 年以上を経過して発症するのかは，いまだ明確にはされていない．しかし，抗 HIV 治療後の CD4 陽性細胞の回復は，まずメモリー T 細胞が増加し始め，6ヵ月後プラトーに達した後に，ナイーブ T 細胞が増加し始めることが指摘されている．メモリー T 細胞の増加する時期には日和見感染症，ナイーブ T 細胞の増加する時期には自己免疫疾患が IRIS として発症すると推察されている[9]．本症例では，Graves 病発症前の保存血清の自己抗体は陰性であり，その後 14ヵ月間に自己抗体が形成されている．しかし，この 14ヵ月間で CD4 陽性細胞数は緩徐な増加がみられるのみで何が Graves 病発症の契機であるかを今後明らかにする必要がある．

わが国ではいまだに AIDS(acquired immunodeficiency syndrome)を発病してから医療機関を受診する症例が多い．しかし，抗 HIV 治療が進歩したので，高度な免疫不全状態であっても免疫状態を回復し，長期生存が可能となっている．そのため，HIV 感染者の治療経過中に IRIS による Graves 病を経験することが増えてくる可能性があり，そのことに留意して診療する必要があると考える．

文　献

1) French MA et al：Zidovudine-induced restoration of cell-mediated immunity to mycobacteria in immunedeficient HIV-infected patients. AIDS 6：1293, 1992
2) Lipman M, Breen R.：Immune reconstitution inflammatory syndrome in HIV. Curr Opin Infect Dis 19：20, 2006
3) Müller M et al：Immune reconstitution inflammatory syndrome in patients starting antiretroviral therapy for HIV infection：a systematic review and meta-analysis. Lancet Infect Dis 10：251, 2010
4) 古西　満ほか：免疫再構築症候群の発症状況調査．厚生労働科学研究費補助金エイズ対策研究事業 HAART 時代の日和見合併症に関する研究 平成 15 年度総括・分担研究報告書，82 頁，2004
5) Gilquin J et al：Delayed occurrence of Graves' disease after immune restoration with HAART. Lancet 352：1907, 1998
6) Crum NF et al：Graves disease：an increasingly recognized immune reconstitution syndrome. AIDS 20：466, 2006
7) 守谷研二ほか：HAART 中の Graves 病を発症した HIV 感染症例．日エイズ会誌 5：158，2003
8) 濱田佳寿ほか：HAART 療法中にバセドウ病を発症した一例．日内分泌会誌 86：286，2010
9) Chen F：Characteristics of autoimmune thyroid disease occurring as a late complication of immune reconstitution in patients with advanced human immunodeficiency virus(HIV)disease. Medicine 84：98, 2005

JCM
Journals.ASM.org

Clinical and Microbiological Differences between *Mycobacterium abscessus* and *Mycobacterium massiliense* Lung Diseases

Toshiyuki Harada,[a] Yasushi Akiyama,[a] Atsuyuki Kurashima,[b] Hideaki Nagai,[c] Kazunari Tsuyuguchi,[d] Takashi Fujii,[e] Syuichi Yano,[f] Eriko Shigeto,[g] Toshihiko Kuraoka,[h] Akira Kajiki,[i] Yoshihiro Kobashi,[j] Fumio Kokubu,[k] Atsuo Sato,[l] Shiomi Yoshida,[m] Tomotada Iwamoto,[n] and Hajime Saito[o]

Center for Respiratory Diseases, Hokkaido Social Insurance Hospital, Sapporo, Japan[a]; Clinical Research Advisor, Japan Anti-Tuberculosis Association, Fukujuji Hospital, Kiyose, Japan[b]; Center for Respiratory Diseases, National Hospital Organization Tokyo National Hospital, Kiyose, Japan[c]; Department of Respiratory Medicine, Clinical Research Center, National Hospital Organization Kinki-Chuo Chest Medical Center, Sakai, Japan[d]; Department of Internal Medicine, Japan Anti-Tuberculosis Association Osaka Branch, Osaka Hospital, Neyagawa, Japan[e]; Department of Pulmonary Medicine, National Hospital Organization Matsue Medical Center, Matsue, Japan[f]; Department of Respiratory Medicine, National Hospital Organization Higashihiroshima Medical Center, Higashihiroshima, Japan[g]; Internal Medicine, Kyosai-Yoshijima Hospital, Hiroshima, Japan[h]; Department of Respiratory Medicine, National Hospital Organization Omuta Hospital, Omuta, Japan[i]; Division of Respiratory Diseases, Department of Medicine, Kawasaki Medical School, Kurashiki, Japan[j]; Department of Respiratory Medicine, Showa University Fujigaoka Hospital, Yokohama, Japan[k]; Respiratory Department, National Hospital Organization Minami-Kyoto Hospital, Jouyou, Japan[l]; Clinical Research Center, National Hospital Organization Kinki-Chuo Chest Medical Centre, Sakai, Japan[m]; Department of Microbiology, Kobe Institute of Health, Kobe, Japan[n]; and Hiroshima Environment & Health Association, Health Science Center, Hiroshima, Japan[o]

In recent years, many novel nontuberculous mycobacterial species have been discovered through genetic analysis. *Mycobacterium massiliense* and *M. bolletii* have recently been identified as species separate from *M. abscessus*. However, little is known regarding their clinical and microbiological differences in Japan. We performed a molecular identification of stored *M. abscessus* clinical isolates for further identification. We compared clinical characteristics, radiological findings, microbiological findings, and treatment outcomes among patients with *M. abscessus* and *M. massiliense* lung diseases. An analysis of 102 previous isolates of *M. abscessus* identified 72 (71%) *M. abscessus*, 27 (26%) *M. massiliense*, and 3 (3%) *M. bolletii* isolates. Clinical and radiological findings were indistinguishable between the *M. abscessus* and *M. massiliense* groups. Forty-two (58%) patients with *M. abscessus* and 20 (74%) patients with *M. massiliense* infections received antimicrobial treatment. Both the *M. abscessus* and *M. massiliense* groups showed a high level of resistance to all antimicrobials, except for clarithromycin, kanamycin, and amikacin. However, resistance to clarithromycin was more frequently observed in the *M. abscessus* than in the *M. massiliense* group (16% and 4%, respectively; $P = 0.145$). Moreover, the level of resistance to imipenem was significantly lower in *M. abscessus* isolates than in *M. massiliense* isolates (19% and 48%, respectively; $P = 0.007$). The proportions of radiological improvement, sputum smear conversion to negativity, and negative culture conversion during the follow-up period were higher in patients with *M. massiliense* infections than in those with *M. abscessus* infections. Patients with *M. massiliense* infections responded more favorably to antimicrobial therapy than those with *M. abscessus* infections.

Mycobacterium species are common causes of pulmonary infections in both humans and animals (14). Although members of the *Mycobacterium tuberculosis* complex cause the majority of pulmonary infections worldwide, many nontuberculous mycobacteria (NTM) can cause similar infections (13, 20). In recent years, many novel NTM species have been discovered through the increased application of genetic investigation tools; detailed genetic characterizations have helped define new taxonomic groupings (17, 29). Recently, two new *M. abscessus*-related species, *M. massiliense* and *M. bolletii*, were identified, which were previously grouped with *M. abscessus* (1, 3). The rate of isolation of these two species has been increasing in Japan. However, very little is known about the natural epidemiology and pathogenicity of *M. massiliense* and *M. bolletii* outside outbreak situations. One report found that the ratio of *M. abscessus* to all NTM is much higher in South Korea (19) than in other countries, including Japan.

Here, we aimed to evaluate the epidemiology, clinical and radiological spectrum, treatments, drug susceptibility, and outcome of *M. abscessus* and *M. massiliense* lung diseases during therapy in Japan.

MATERIALS AND METHODS

Study population. We retrospectively reviewed the medical records of patients initially diagnosed with *M. abscessus* lung disease according to the 2007 American Thoracic Society/Infectious Diseases Society of America (ATS/IDSA) guidelines (16) between January 1990 and December 2010 at 12 hospitals or institutions in Japan. These *M. abscessus* species were thereafter identified as *M. abscessus*, *M. massiliense*, and *M. bolletii*. Clinical, radiological, microbiological, management, and outcome data were collected from medical files. Permission was obtained from the institutional review board committee of Hokkaido Social Insurance Hospital (approval number 2011-11). Informed consent was waived because of the retrospective nature of the study.

Received 9 May 2012 Returned for modification 24 July 2012
Accepted 14 August 2012
Published ahead of print 22 August 2012
Address correspondence to Toshiyuki Harada, t-harada@hok-shaho-hsp.jp.
Supplemental material for this article may be found at http://jcm.asm.org/.
Copyright © 2012, American Society for Microbiology. All Rights Reserved.
doi:10.1128/JCM.01175-12